

Pyrazolo[4,3-*e*]1,2,4-triazolo[1,5-*c*]pyrimidine Derivatives as Highly Potent and Selective Human A₃ Adenosine Receptor Antagonists: Influence of the Chain at the N⁸ Pyrazole Nitrogen

Pier Giovanni Baraldi,^{*,§} Barbara Cacciari,[§] Romeo Romagnoli,[§] Giampiero Spalluto,[†] Stefano Moro,[#] Karl-Norbert Klotz,[‡] Edward Leung,^{||} Katia Varani,[‡] Stefania Gessi,[‡] Stefania Merighi,[‡] and Pier Andrea Borea[‡]

Dipartimento di Scienze Farmaceutiche and Dipartimento di Medicina Clinica e Sperimentale-Sezione di Farmacologia, Università degli Studi di Ferrara, Via Fossato di Mortara 17-19, I-44100 Ferrara, Italy; Dipartimento di Scienze Farmaceutiche, Università degli Studi di Trieste, Piazzale Europa 1, I-34127 Trieste, Italy; Molecular Modeling Section, Dipartimento di Scienze Farmaceutiche, Università di Padova, Via Marzolo 5, I-35131 Padova, Italy; Institut für Pharmakologie, Universität Würzburg, Versbacher Strasse 9, D-97078 Würzburg, Germany; and Medco Research, Research Triangle Park, North Carolina 27709

Received July 31, 2000

An enlarged series of pyrazolotriazolopyrimidines previously reported, in preliminary form (Baraldi et al. *J. Med. Chem.* **1999**, 42, 4473–4478), as highly potent and selective human A₃ adenosine receptor antagonists is described. The synthesized compounds showed A₃ adenosine receptor affinity in the sub-nanomolar range and high levels of selectivity evaluated in radioligand binding assays at human A₁, A_{2A}, A_{2B}, and A₃ adenosine receptors. In particular, the effect of the chain at the N⁸ pyrazole nitrogen was analyzed. This study allowed us to identify the derivative with the methyl group at the N⁸ pyrazole combined with the 4-methoxyphenylcarbamoyl moiety at the N⁵ position as the compound with the best binding profile in terms of both affinity and selectivity (hA₃ = 0.2 nM, hA₁/hA₃ = 5485, hA_{2A}/hA₃ = 6950, hA_{2B}/hA₃ = 1305). All the compounds proved to be full antagonists in a specific functional model where the inhibition of cAMP generation by IB-MECA was measured in membranes of CHO cells stably transfected with the human A₃ receptor. The new compounds are among the most potent and selective A₃ antagonists so far described. The derivatives with higher affinity at human A₃ adenosine receptors proved to be antagonists, in the cAMP assay, capable of inhibiting the effect of IB-MECA with IC₅₀ values in the nanomolar range, with a trend strictly similar to that observed in the binding assay. Also a molecular modeling study was carried out, with the aim to identify possible pharmacophore maps. In fact, a sterically controlled structure–activity relationship was found for the N⁸ pyrazole substituted derivatives, showing a correlation between the calculated molecular volume of pyrazolo[4,3-*e*]1,2,4-triazolo[1,5-*c*]pyrimidine derivatives and their experimental *K_i* values.

Introduction

The actions of adenosine are mediated through G-coupled receptors that are classified into four different subtypes, named A₁, A_{2A}, A_{2B}, and A₃, based on pharmacological criteria and coupling to adenylyl cyclase.^{1,2} While the adenosine A₁ and A_{2A} receptor subtypes have been pharmacologically characterized through the use of selective ligands,³ the A₃ and A_{2B} subtypes are still under investigation.

The adenosine A₃ receptor has been recently cloned from a rat testis cDNA library⁴ and is the subject of intensive pharmacological characterization. The adenosine A₃ receptors have now also been cloned from several other species such as human,^{5,6} sheep,⁷ mouse,⁸ and rabbit.⁹ Significant differences in sequence homology

(72%) for the A₃ receptors have been observed between species.^{10,11} The rat A₃ adenosine receptor in particular behaves anomalously in ligand binding assays. For these reasons, the hypothesis of the existence of two different adenosine A₃ receptor subtypes has been proposed, but the question has not yet been answered.¹²

Activation of adenosine A₃ receptors has been shown to stimulate phospholipase C¹³ and D¹⁴ and to inhibit adenylyl cyclase.³ Activation of A₃ adenosine receptors in the rat results in hypotension, by promotion of release of inflammatory mediators from mast cells.¹⁵ It has also been suggested that the A₃ receptor plays an important role in brain ischemia,^{16,17} immunosuppression,¹⁸ and bronchospasm in several animal models.^{19a} On these pharmacological observations, highly selective A₃ adenosine receptor antagonists are being sought as potential antiasthmatic,^{19b} antiinflammatory, and cerebroprotective agents.^{10,20} In the past few years, different classes of compounds with nonxanthine structures have been reported to be A₃ adenosine receptor antagonists:²¹ dihydropyridine and pyridine analogues,^{22–26} flavonoid,^{27,28} isoquinoline,^{29–31} and triazoloquinazoline derivatives.^{32–33}

* To whom correspondence should be addressed. Phone: +39-(0)-532-291293. Fax: +39-(0)532-291296. E-mail: pgb@dns.unife.it.

[§] Dipartimento di Scienze Farmaceutiche, Università degli Studi di Ferrara.

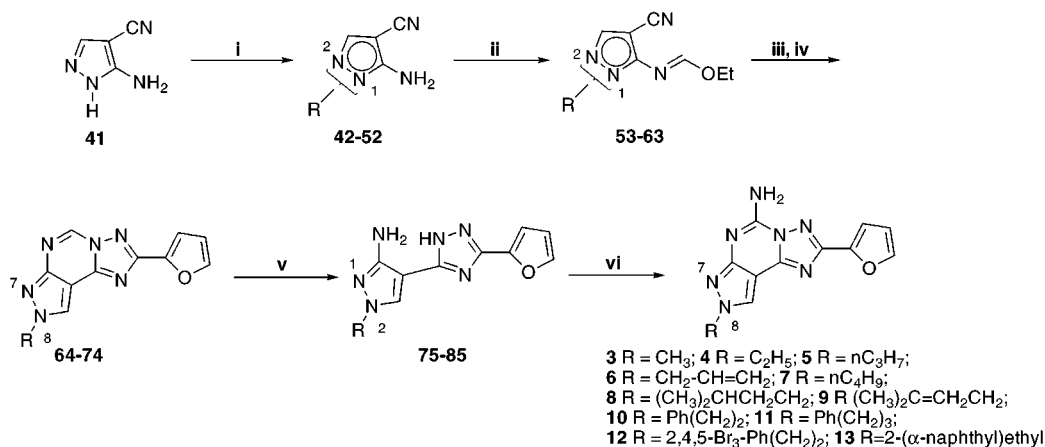
[‡] Dipartimento di Medicina Clinica e Sperimentale-Sezione di Farmacologia, Università degli Studi di Ferrara.

[†] Università degli Studi di Trieste.

[#] Università di Padova.

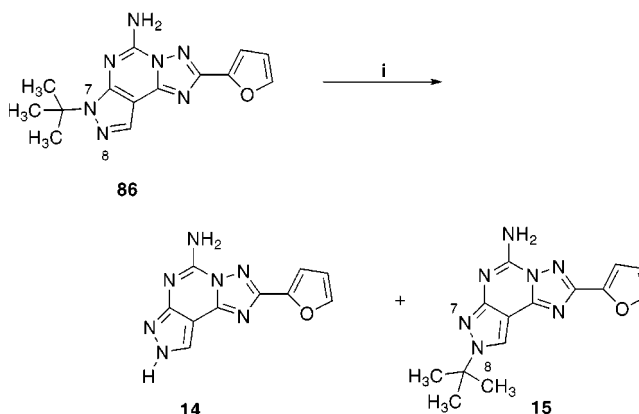
[‡] Universität Würzburg.

^{||} Medco Research.

Scheme 1^a

^a Reagents: (i) NaH, DMF, RX; (ii) HC(OEt)₃, reflux; (iii) 2-furoic hydrazide, MeO(CH₂)₂OH; (iv) Ph₂O, 260 °C, flash chromatography; (v) HCl, reflux; (vi) NH₂CN, 1-methyl-2-pyrrolidone, pTsoH, 140 °C.

In this field of research, our group has recently reported, in preliminary form, a new series of pyrazolo[4,3-*e*]1,2,4-triazolo[1,5-*c*]pyrimidine derivatives as highly potent and selective human A₃ adenosine receptor antagonists.³⁴ In particular two of these compounds, 5-[[[(4-methoxyphenyl)amino]carbonyl]amino-8-ethyl-2-(2-furyl)pyrazolo[4,3-*e*]1,2,4-triazolo[1,5-*c*]pyrimidine (**1**) and 5-[[[(4-methoxyphenyl)amino]carbonyl]amino-8-*n*-propyl-2-(2-furyl)pyrazolo[4,3-*e*]1,2,4-triazolo[1,5-*c*]pyrimidine (**2**), proved to be the most potent and selective adenosine A₃ antagonists in humans ever reported, while proving ineffective in a rat model. The design of these derivatives was based on the formation of hybrid molecules between the 3-chloro- or 4-methoxyphenyl-carbamoyl moieties present in A₃ agonists^{35,36} and the nucleus of A_{2A} antagonists^{37–40} previously reported by our group.

Scheme 2^a

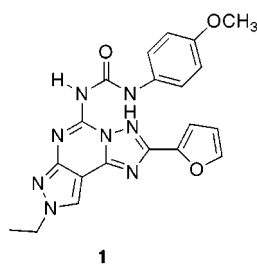
^a Reagents: (i) 99% HCOOH, 130 °C, 48 h.

the chain at the N⁸ position has been modified in order to optimize the steric and lipophilic characteristics of this moiety for the recognition of the human A₃ adenosine receptor subtype. In addition, on the basis of the studies previously reported by Jacobson and co-workers, we investigated the effect of a phenylcarbamoyl chain on the interaction with A₃ adenosine receptors, introducing it on the amino function present in the 5-amino-9-chloro-2-(2-furyl)[1,2,4]triazolo[1,5-*c*]quinazoline (CGS-15943) which possesses affinity for the human A₃ adenosine receptor (*K_i* hA₃ 90 nM).³²

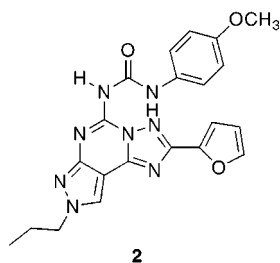
Chemistry

Compounds **1–40** were prepared following the general synthetic strategy summarized in Schemes 1 and 3. Compounds **1–40** were synthesized according to a well-known procedure for the synthesis of the pyrazolo[4,3-*e*]1,2,4-triazolo[1,5-*c*]pyrimidines, previously reported³⁹ (Table 1).

Alkylation of 5-amino-4-cyanopyrazole **41** with the appropriate alkyl halide in dry dimethylformamide led to an approximately 1:4 mixture of the N¹ and N² regioisomers **42–52** as an inseparable mixture, used for the following steps without any further purification³⁴ (Scheme 1). Pyrazoles **42–52** were transformed into the corresponding imidates **53–63** through refluxing in triethyl orthoformate. The imino ethers **53–63** were reacted with 2-furoic hydrazide in refluxing 2-methoxy-

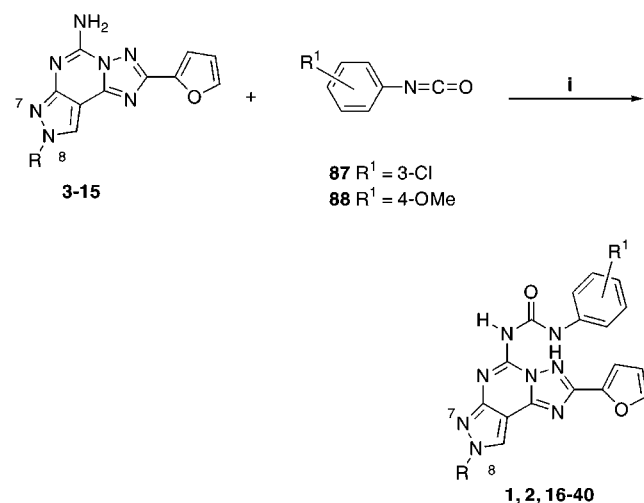


hA₁ = 1,026 nM; hA_{2A} = 1,045 nM; hA₃ = 0.28 nM
 hA₁/hA₃ = 3,664; hA_{2A}/hA₃ = 3,732



hA₁ = 1,197 nM; hA_{2A} = 141 nM; hA₃ = 0.29 nM
 hA₁/hA₃ = 4,128; hA_{2A}/hA₃ = 486

In this fully detailed version, we wish to report all the synthesized compounds (**1–40**) of this series, in which the substituent on the phenyl ring (3-chloro or 4-methoxy) at the 5-position has been maintained while

Scheme 3^a^a Reagents: (i) THF, reflux, 12 h.

ethanol to provide the pyrazolo[3,4-*d*]pyrimidine intermediates. These were converted through a thermally induced cyclization in diphenyl ether to the desired derivatives **64–74** in good overall yield (50–63%), after separation of *N*⁷ (minor product) and *N*⁸ (major product) regioisomers by flash chromatography.³⁴ Hydrolysis with aqueous 10% HCl afforded the aminotriazoles **75–85**, which were in turn converted into the 5-amino-8-(substituted)-2-(2-furyl)pyrazolo[4,3-*e*]1,2,4-triazolo[1,5-*c*]pyrimidine derivatives **3–13**.

The unsubstituted (**14**) and *N*⁸-*tert*-butyl (**15**) derivatives were prepared by treatment of the corresponding *N*⁷-*tert*-butyl derivative **86**, by treatment with 99% formic acid at 130 °C for 48 h. These reaction conditions afforded a separable mixture of **14** and **15**³⁷ (Scheme 2).

The urea derivatives **1, 2**, and **16–40** were obtained by a coupling reaction of derivatives **3–15** with the

Table 1. Structures and Physicochemical Parameters of the Synthesized Compounds

compd	R	R ¹	mp (°C)	MW	formula	anal.
14	H	H	245 dec	241.07	C ₁₀ H ₇ N ₇ O	C, H, N
16	H	4-MeO-Ph-NHCO	249–250	390.11	C ₁₈ H ₁₄ N ₈ O ₃	C, H, N
17	H	3-Cl-Ph-NHCO	276–277	394.06	C ₁₇ H ₁₁ N ₈ O ₂ Cl	C, H, N
3	CH ₃	H	167–168	255.24	C ₁₁ H ₉ N ₇ O	C, H, N
18	CH ₃	4-MeO-Ph-NHCO	193–195	404.39	C ₁₉ H ₁₆ N ₈ O ₃	C, H, N
19	CH ₃	3-Cl-Ph-NHCO	142–145	408.80	C ₁₈ H ₁₃ N ₈ O ₂ Cl	C, H, N
4	C ₂ H ₅	H	249–250	269.26	C ₁₂ H ₁₁ N ₇ O	C, H, N
1	C ₂ H ₅	4-MeO-Ph-NHCO	200–201	418.41	C ₂₀ H ₁₈ N ₈ O ₃	C, H, N
20	C ₂ H ₅	3-Cl-Ph-NHCO	204–205	422.83	C ₁₉ H ₁₅ N ₈ O ₂ Cl	C, H, N
5	<i>n</i> -C ₃ H ₇	H	209–210	283.29	C ₁₃ H ₁₃ N ₇ O	C, H, N
2	<i>n</i> -C ₃ H ₇	4-MeO-Ph-NHCO	146–148	432.44	C ₂₁ H ₂₀ N ₈ O ₃	C, H, N
21	<i>n</i> -C ₃ H ₇	3-Cl-Ph-NHCO	138–139	436.86	C ₂₀ H ₁₇ N ₈ O ₂ Cl	C, H, N
6	CH ₂ -CH=CH ₂	H	207–209	281.27	C ₁₃ H ₁₁ N ₇ O	C, H, N
22	CH ₂ -CH=CH ₂	4-MeO-Ph-NHCO	180	430.15	C ₂₁ H ₁₈ N ₈ O ₃	C, H, N
7	<i>n</i> -C ₄ H ₉	H	200–203	297.32	C ₁₄ H ₁₅ N ₇ O	C, H, N
23	<i>n</i> -C ₄ H ₉	4-MeO-Ph-NHCO	197–198	446.47	C ₂₂ H ₂₂ N ₈ O ₃	C, H, N
24	<i>n</i> -C ₄ H ₉	3-Cl-Ph-NHCO	210–212	450.89	C ₂₁ H ₁₉ N ₈ O ₂ Cl	C, H, N
15	<i>t</i> -C ₄ H ₉	H	108–110	297.13	C ₁₄ H ₁₅ N ₇ O	C, H, N
25	<i>t</i> -C ₄ H ₉	4-MeO-Ph-NHCO	198–203 dec	446.18	C ₂₂ H ₂₂ N ₈ O ₃	C, H, N
26	<i>t</i> -C ₄ H ₉	3-Cl-Ph-NHCO	203–206	450.13	C ₂₁ H ₁₉ N ₈ O ₂ Cl	C, H, N
8	(CH ₃) ₂ CH-CH ₂ -CH ₂	H	212–213	311.34	C ₁₅ H ₁₇ N ₇ O	C, H, N
27	(CH ₃) ₂ CH-CH ₂ -CH ₂	4-MeO-Ph-NHCO	192–193	460.49	C ₂₃ H ₂₄ N ₈ O ₃	C, H, N
28	(CH ₃) ₂ CH-CH ₂ -CH ₂	3-Cl-Ph-NHCO	199–200	464.91	C ₂₂ H ₂₁ N ₈ O ₂ Cl	C, H, N
9	(CH ₃) ₂ C=CH-CH ₂	H	178–179	309.33	C ₁₅ H ₁₅ N ₇ O	C, H, N
29	(CH ₃) ₂ C=CH-CH ₂	4-MeO-Ph-NHCO	198–199	458.48	C ₂₃ H ₂₂ N ₈ O ₃	C, H, N
30	(CH ₃) ₂ C=CH-CH ₂	3-Cl-Ph-NHCO	204–205	462.90	C ₂₂ H ₁₉ N ₈ O ₂ Cl	C, H, N
10	Ph-CH ₂ -CH ₂	H	183–185	345.36	C ₁₈ H ₁₅ N ₇ O	C, H, N
31	Ph-CH ₂ -CH ₂	4-MeO-Ph-NHCO	180–181	494.51	C ₂₆ H ₂₂ N ₈ O ₃	C, H, N
32	Ph-CH ₂ -CH ₂	3-Cl-Ph-NHCO	186–187	498.93	C ₂₅ H ₁₉ N ₈ O ₂ Cl	C, H, N
11	Ph-CH ₂ -CH ₂ -CH ₂	H	168–170	359.39	C ₁₉ H ₁₇ N ₇ O	C, H, N
33	Ph-CH ₂ -CH ₂ -CH ₂	4-MeO-Ph-NHCO	174–175	508.54	C ₂₇ H ₂₄ N ₈ O ₃	C, H, N
34	Ph-CH ₂ -CH ₂ -CH ₂	3-Cl-Ph-NHCO	183–184	512.96	C ₂₆ H ₂₁ N ₈ O ₂ Cl	C, H, N
12	2,4,5-Br ₃ -Ph-CH ₂ -CH ₂	H	145–146	578.86	C ₁₈ H ₁₂ N ₇ OBr ₃	C, H, N
35	2,4,5-Br ₃ -Ph-CH ₂ -CH ₂	4-MeO-Ph-NHCO	155	727.91	C ₂₆ H ₁₉ N ₈ O ₃ Br ₃	C, H, N
36	2,4,5-Br ₃ -Ph-CH ₂ -CH ₂	3-Cl-Ph-NHCO	158–160	731.86	C ₂₅ H ₁₆ N ₈ O ₂ Br ₃ Cl	C, H, N
13	2-(α-naphthyl)ethyl	H	175–177	397.16	C ₂₂ H ₁₉ N ₇ O	C, H, N
37	2-(α-naphthyl)ethyl	4-MeO-Ph-NHCO	187–188	546.21	C ₃₀ H ₂₆ N ₈ O ₃	C, H, N
38	2-(α-naphthyl)ethyl	3-Cl-Ph-NHCO	195–196	551.01	C ₂₉ H ₂₃ N ₈ O ₂ Cl	C, H, N
39		4-MeO-Ph-NHCO	216–217	434.84	C ₂₁ H ₁₅ N ₆ O ₃ Cl	C, H, N
40		3-Cl-Ph-NHCO	212–213	439.26	C ₂₀ H ₁₂ N ₆ O ₂ Cl ₂	C, H, N

commercially available isocyanates **87** and **88**^{35,36} (Scheme 3).

Results and Discussion

Table 2 gives the receptor binding affinities of compounds **1**, **2**, and **16–40** and the corresponding N⁵ unsubstituted derivatives **3–15**, determined at human A₁, A_{2A}, A_{2B}, and A₃ receptors expressed in CHO (A₁, A_{2A}, A₃) or HEK-293 (A_{2B}) cells.

[³H]-1,3-Dipropyl-8-cyclopentylxanthine ([³H]DPC-PX)^{41,42} (A₁, A_{2B}), [³H]-5-amino-7-(2-phenylethyl)-2-(2-furyl)pyrazolo[4,3-*e*]1,2,4-triazolo[1,5-*c*]pyrimidine ([³H]-SCH 58261) (A_{2A}),⁴³ and [³H]-5-(4-methoxyphenylcarbamoyl)amino-8-propyl-2-(2-furyl)pyrazolo[4,3-*e*]1,2,4-triazolo[1,5-*c*]pyrimidine ([³H]MRE3008-F20) (A₃)⁴² were used as radioligands in binding assays.

As previously observed, it is clearly evident that compounds with the free amino group at the N⁵ position (**3–5**, **7–15**) show high affinity for both A₁ and A_{2A} receptors and surprisingly also for the human A_{2B} subtype with different degrees of selectivity.³⁴ In particular compounds with a long alkyl chain (**8**, **9**) or a phenylethyl moiety (**10**) showed the best binding profile at human A_{2B} receptors (5–12 nM) but, unfortunately, resulted ineffective at human A₃ adenosine receptors (micromolar range) while having high affinity for A₁ and A_{2A} subtypes (0.3–5 nM).

The compounds with the 2-phenylethyl (**10**) and 3-phenylpropyl (**11**) chains at the pyrazole nitrogen show the best profile at the human A_{2A} adenosine receptor (0.16–0.34 nM) but low selectivity versus A₁ and A_{2B} receptor subtypes. These two derivatives are the regioisomers of two of the most potent and selective A_{2A} antagonists, named SCH 58261 and SCH 63390, previously reported.³⁹ These data confirm the importance of the position of the chain in discriminating the affinities at different receptor subtypes.

These N⁵ unsubstituted derivatives, in general, were ineffective at the human A₃ adenosine receptors, but interestingly, compounds with small alkyl or aralkyl chains (e.g. compounds **3–5**, **10**, **11**) or hydrogen (**14**) at the pyrazole nucleus showed slightly better affinity toward human A₃ receptors (300–400 nM) with respect to compounds with a bulky aralkyl chain (e.g. compounds **12**, **13**: hA₃ > 3 μM).

As previously observed, when the substituted phenylcarbamoyl chain is present at the N⁵ position all the synthesized derivatives **1**, **2**, and **16–40** show affinities in the nanomolar range toward human A₃ receptors with a different degree of selectivity versus the other receptor subtypes.³⁴ In particular in all the examples shown in Table 2, it is evident that the 4-methoxyphenylcarbamoyl moiety (e.g. compounds **1**, **2**, **16**, **18**, **25**) confers higher affinity to the human A₃ receptor than the 3-chlorophenylcarbamoyl chain (e.g. compounds **20**, **21**, **17**, **19**, **26**) with a difference of about 2–10-fold. On the contrary, in some cases, the presence of 3-chloro substitution on the phenyl ring (e.g. compounds **17**, **21**, **24**) seems to produce an increased affinity toward human A_{2B} receptors of about 5–40-fold with respect to the 4-methoxy substituted derivatives (e.g. compounds **16**, **18**, **2**, **23**), with a concomitant decrease in selectivity for the human A₃ adenosine receptor subtype.

Analyzing this enlarged series of compounds, it is evident that small chains on N⁸ of the pyrazole produce

the best compounds in term of both affinity and selectivity. In fact the N⁸ unsubstituted (**16**), methyl (**18**), ethyl (**1**), propyl (**2**), and butyl (**23**) derivatives showed affinity values in the sub-nanomolar range (0.14–0.8 nM) and high selectivity versus the other receptor subtype (200–7000). From these results, it seems evident that small chains, in particular methyl substitution, together with the 4-methoxyphenylcarbamoyl moiety are indispensable for obtaining derivatives with high potency and selectivity. In fact, compound **18** resulted as not only one of the most potent but also the most selective compounds (hA₃ = 0.2 nM, hA₁/hA₃ = 5485, hA_{2A}/hA₃ = 6950, hA_{2B}/hA₃ = 1305) ever reported. Also comparing this derivative with the previously reported compound **1**,³⁴ an improvement in both affinity and selectivity was obtained.

A different biological profile was observed when the phenylethyl (**31**, **32**) and phenylpropyl (**33**, **34**) chains were introduced; in fact, a reduction in affinity of about 10–100-fold is evident (e.g. compound **2**: hA₃ = 0.80 nM vs compound **33**: hA₃ = 40 nM). This effect could be attributed to both the steric and lipophilic contributions of the chain.

When branched chains such as isopentyl (**27**, **28**) or 2-isopentenyl (**29**, **30**) were introduced on the pyrazole nitrogen, a significant loss in both affinity and selectivity was observed. But, when the steric bulk is close to the pyrazole nitrogen, as in the case of the *tert*-butyl moiety (**25**, **26**) affinity and selectivity were well retained. These results suggest that the steric factor (in particular when the bulky group is far from the pyrazole nitrogen) is more important than the lipophilic one. To support this hypothesis, we synthesized derivatives **35–38**, in which the 2-(α -naphthyl)ethyl and 2,4,5-tribromophenylethyl moieties were introduced on the pyrazole nitrogen. From the data reported in Table 2 it appears evident that the compounds with the 2-(α -naphthyl)ethyl chain (**37**, **38**), in which the steric factor is unaltered while the lipophilic character is increased, have a slight decrease in affinity but retention of good selectivity. On the contrary, for derivatives **35** and **36** in which both steric and lipophilic factors are increased, a dramatic reduction of affinity and selectivity was observed. Another interesting aspect, the rigidity of the chain at the N⁸ position, was investigated by introducing unsaturated chains such as allyl (**22**) or 2-isopentenyl (**29**, **30**). As summarized in Table 2 it is evident that more rigid chains do not improve both affinity and selectivity toward human A₃ adenosine receptors with respect to saturated chains (e.g. **27**, **28** vs **29**, **30** and/or **2** vs **22**). On the other hand, these derivatives represent useful precursors for the preparation of tritiated radioligands, as recently reported by our group for derivative **22**. Reduction of the double bond in **22** with tritium gas resulted in the tritiated form of compound **2**, well-characterized as the first radioligand antagonist for human A₃ adenosine receptors, named [³H]MRE3008-F20.^{42,44} With the aim to better investigate the effect of the phenylcarbamoyl chain on affinity toward human A₃ adenosine receptors, we introduced these chains on the amino group of CGS15943 (compounds **39**, **40**) following the same rationale suggested by Jacobson and co-workers for the synthesis of 9-chloro-2-(2-furyl)-5-

Table 2. Binding Affinity at hA₁, hA_{2A}, hA_{2B}, and hA₃ Adenosine Receptors of the Synthesized Compounds

compd	<i>K_i</i> (nM)				hA ₁ /hA ₃	hA _{2A} /hA ₃	hA _{2B} /hA ₃
	hA ₁ ^a	hA _{2A} ^b	hA _{2B} ^c	hA ₃ ^d			
14	140 (123–160)	20 (17–24)	51 (44–58)	348 (267–453)	0.40	0.06	0.15
16	448 (365–550)	520 (484–558)	350 (332–369)	0.14 (0.08–0.27)	3200	3715	2500
17	238 (179–317)	248 (218–283)	70 (61–80)	0.50 (0.34–0.73)	476	496	140
3	101 (81–127)	2.80 (2.40–3.55)	90 (81–101)	300 (265–339)	0.33	0.009	0.30
18	1097 (928–1297)	1390 (1220–1590)	261 (226–301)	0.20 (0.17–0.24)	5485	6950	1305
19	350 (323–378)	1195 (1024–1396)	205 (157–268)	0.40 (0.24–0.64)	875	2987	512
4	5.00 (4.05–6.20)	1.95 (1.70–2.10)	65 (56–75)	331 (285–385)	0.015	0.005	0.19
1	1026 (785–1341)	1040 (830–1310)	245 (188–320)	0.60 (0.51–0.70)	1710	1733	408
20	249 (215–289)	180 (160–210)	150 (107–210)	1.60 (1.42–1.79)	155	112	93.7
5	10 (7–14)	2.51 (1.90–3.37)	39 (35–45)	408 (364–460)	0.024	0.006	0.095
2	1197 (1027–1396)	140 (120–155)	2056 (1637–2582)	0.80 (0.63–0.1.00)	1496	175	2570
21	30 (23–40)	1220 (880–1682)	57 (50–63)	0.91 (0.85–0.98)	33	1340	62.6
22	1531 (1354–1372)	176 (150–207)	2030 (1770–2327)	0.48 (0.32–0.74)	3189	366	4229
7	14 (11–17)	1.60 (1.4–2.1)	53 (40–69)	600 (525–691)	0.02	0.002	0.09
23	296 (269–326)	80 (65–92)	303 (260–352)	0.32 (0.27–0.34)	925	250	946
24	245 (213–281)	95 (70–130)	70 (56–89)	0.60 (0.52–0.68)	408	158	116
15	175 (134–229)	45 (36–55)	400 (343–468)	1149 (1061–1245)	0.15	0.04	0.35
25	796 (632–1003)	545 (461–645)	1715 (1531–1920)	0.80 (0.63–1.00)	995	681	2144
26	1015 (885–1163)	796 (632–1003)	450 (432–469)	2.78 (2.13–3.62)	365	286	162
8	2.00 (1.72–2.36)	0.78 (0.60–1.00)	9.1 (7.4–11.3)	700 (664–738)	0.002	0.001	0.013
27	175 (149–204)	65 (47–78)	54 (45–64)	30 (23–40)	5.8	2.16	1.80
28	100 (83–120)	115 (85–164)	61 (55–68)	40 (33–48)	2.5	2.87	1.5
9	5.42 (4.72–6.23)	0.80 (0.65–1.06)	12 (8–18)	811 (691–952)	0.006	0.0009	0.014
29	300 (254–356)	1025 (850–1230)	58 (52–65)	40 (35–47)	7.5	25.6	1.45
30	352 (329–375)	110 (85–140)	81 (70–94)	55 (50–61)	6.4	2.0	1.47
10	1.00 (0.66–1.51)	0.34 (0.22–0.44)	5.1 (3.9–6.7)	280 (247–317)	0.003	0.001	0.0017
31	201 (172–236)	120 (100–145)	81 (70–94)	0.98 (1.22–1.78)	205	122	82.6
32	251 (229–276)	105 (90–125)	90 (81–101)	8.0 (7.2–8.9)	6.3	13	11.2
11	3.00 (2.65–3.39)	0.16 (0.06–0.48)	49 (38–63)	430 (378–488)	0.007	0.0004	0.011
33	251 (221–286)	1010 (880–1160)	802 (719–895)	40 (33–48)	6.27	25.2	20
34	1500 (1325–1693)	200 (185–210)	226 (183–278)	60 (51–70)	25	3.3	3.7
12	247 (170–358)	348 (267–453)	1113 (934–1327)	4481 (3650–5501)	0.06	0.08	0.25
35	255 (191–339)	2030 (1770–2327)	>10000	25 (17–36)	10.2	81.2	>400
36	389 (327–462)	3600 (3420–3788)	1816 (1681–1961)	71 (65–78)	5.50	51	26
13	348 (267–453)	896 (730–1100)	4294 (3828–4817)	3416 (3228–3614)	0.10	0.26	1.26
37	2466 (2362–2575)	3260 (2826–3761)	>10000	16 (14–19)	154	204	>625
38	3164 (2894–3460)	>10000	>10000	51 (34–76)	62	>196	>196
CGS15943	4.4 (4.1–4.7)	0.43 (0.37–0.49)	23 (18–29)	85 (76–95)	0.05	0.005	0.27
39	7.6 (6.5–8.7)	9.4 (8.7–10.2)	22 (19–27)	0.14 (0.08–0.24)	43	50	158
40	8.1 (6.9–9.7)	9.5 (8.7–10.5)	30 (23–40)	0.19 (0.13–0.27)	54	67	157

^a Displacement of specific [³H]DPCPX binding at human A₁ receptors expressed in CHO cells (*n* = 3–6). ^b Displacement of specific [³H]SCH 58261 binding at human A_{2A} receptors expressed in CHO cells (*n* = 3–6). ^c Displacement of specific [³H]DPCPX binding at human A_{2B} receptors expressed in HEK-293 cells (*n* = 3–6). ^d Displacement of specific [³H]MRE3008-F20 binding at human A₃ receptors expressed in CHO cells (*n* = 3–6). Data are expressed as geometric means with 95% confidence limits.

[(phenylacetyl)amino][1,2,4]triazolo[1,5-*c*]quinazoline (MRS1220).³²

The binding data of these derivatives followed the same profile observed for the pyrazolic series. In fact the introduction of substituted-phenylcarbamoyl chains at the N⁵ position induced an increase of potency at the human A₃ adenosine receptors ($hA_3 = 0.14\text{--}0.19\text{ nM}$) with respect to the unsubstituted compound CGS15943 ($hA_3 = 85\text{ nM}$), on the contrary the synthesized compounds showed low selectivity versus other receptor subtypes if compared with the pyrazolic series. These results allow us to hypothesize that, while the substituted-phenylcarbamoyl moiety confers potency at the human A₃ adenosine receptors, small chains on the pyrazole nucleus and probably the nitrogens present on the heterocycle permit to discriminate the affinity to human A₃ adenosine receptors versus other receptor subtypes. In fact, from a comparison between compound **16** ($hA_3 = 0.14\text{ nM}$, $hA_1/hA_3 = 3200$, $hA_{2A}/hA_3 = 3715$, $hA_{2B}/hA_3 = 2500$) or **18** ($hA_3 = 0.2\text{ nM}$, $hA_1/hA_3 = 5485$, $hA_{2A}/hA_3 = 6950$, $hA_{2B}/hA_3 = 1305$) with compound **39** ($hA_3 = 0.14\text{ nM}$, $hA_1/hA_3 = 43$, $hA_{2A}/hA_3 = 50$, $hA_{2B}/hA_3 = 158$) it is clearly evident these compounds cover the same range of affinity at human A₃ adenosine receptors but differ significantly in terms of selectivity in favor of pyrazolic derivatives. From these experimental observations, it is possible to hypothesize that not only small chains possess the ideal, steric and probably lipophilic, characteristics for interaction with the human adenosine A₃ receptor subtype but also the nitrogens present on the pyrazole nucleus play an important role for receptor interaction. To better rationalize these experimental observations, a molecular modeling study was carried out to identify a possible pharmacophore map. Moro et al. recently developed a model of the human A₃ receptor, using rhodopsin as a template, by adapting a facile method to simulate the reorganization of the native receptor structure induced by the ligand coordination (cross-docking procedure).⁴⁵ As already reported, the recognition of classic A₃ antagonists appears to occur in the upper region of the transmembrane helical bundle.⁴⁵ TMs 3, 5, 6, and 7 seem to be crucial for the recognition of both agonists and antagonists.⁴⁵ Accordingly, the pyrazolo[4,3-*e*]1,2,4-triazolo[1,5-*c*]pyrimidine nucleus should be most favorably oriented perpendicular to the plane of the lipid bilayer, with the carbamoyl moiety at the N⁵ position in proximity to Ser275 (TM7) and the oxygen atom of the 2-(2-furyl) group close to Asn250 (TM6). Two important hydrophilic interactions, probably hydrogen-bonding interactions, seem to be involved between the two ester group and these two polar amino acids. In addition, two hydrophobic pockets are likely present around the N⁸ pyrazole position where an alkyl/aryl side chain would bind (Leu90, TM3; Phe182, TM5) and around the 2-position where the furyl ring would bind (Leu90, TM3; Ile186, TM5). Moreover, a sterically controlled structure–activity relationship (SAR) was found for the N⁸ pyrazole substituted derivatives. As shown in Figure 1, there is a significative correlation between the calculated molecular volume of pyrazolo[4,3-*e*]1,2,4-triazolo[1,5-*c*]pyrimidine derivatives and their experimental K_i values.

In particular A₃ affinities decrease with the increasing molecular volume values at the N⁸ position. As already

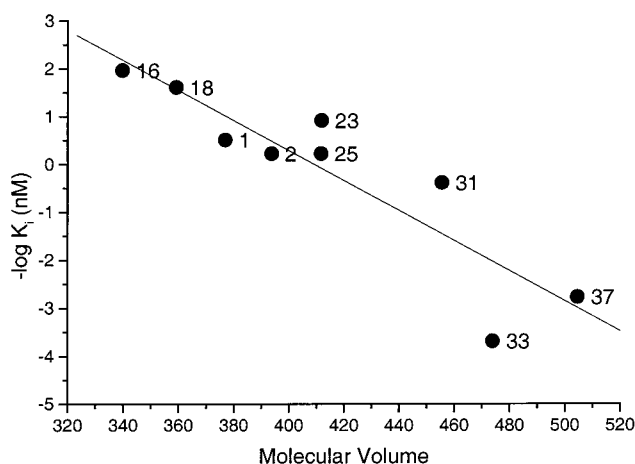


Figure 1. Relationship between molecular volume values and human A₃ affinities (K_i , nM) for the tested pyrazolo[4,3-*e*]1,2,4-triazolo[1,5-*c*]pyrimidine derivatives.

mentioned, a small hydrophobic pocket is present around the N⁸ pyrazole position (Leu90, TM3; Phe182, TM5), and consequently the dimension of the N⁸ pyrazole substituent has to fit very well with the shape of the receptor pocket. In fact, as clearly shown in Table 2, bulky substituents at the N⁸ position are not well-tolerated in the pyrazolo[4,3-*e*]1,2,4-triazolo[1,5-*c*]pyrimidine series. The pharmacophore maps can be summarized as shown in Figure 2. This pharmacophore model fits well with the binding site model in the transmembrane region, based on a variety of human A₃ receptor antagonists, that has been recently proposed.

All of the synthesized compounds were also found to be functional antagonists in a specific functional model where the inhibition of cAMP generation by IB-MECA was measured in membranes of CHO cells stably transfected with the human A₃ receptor (Table 3).⁴⁶

As expected, all the derivatives are full antagonists with different degrees of potency. Compounds **3–5** and **7–15**, with a free amino group at the 5-position, as observed in binding studies, showed poor activity, inhibiting the effect of 100 nM IB-MECA in a range of 3–28% at 1 μM concentration. On the contrary, the N⁵ substituted compounds (**1**, **2**, **16–40**) were more potent in the functional assay than the unsubstituted derivatives (**3–5**, **7–15**).

The derivatives with higher affinity at human A₃ adenosine receptors (e.g. compounds **16**, **18**) proved to be antagonists capable of inhibiting the effect of IB-MECA, with a potency strictly corresponding to that observed in the binding assay. In particular, the derivatives with a binding affinity close to or less than 1 nM inhibit the effect of 100 nM IB-MECA at 1 μM concentration from 68% to 98%, displaying IC_{50} values in the nanomolar range (1.8–14 nM) as observed by inhibition curves for compounds **16**, **18**, **21**, **22**, **2**, and **31** (Figure 3). On the contrary, derivatives with binding affinities higher than 2 nM at human A₃ adenosine receptors (e.g. compounds **15**, **26–28**) inhibit the effect of 100 nM IB-MECA in a range of 32–70% at 1 μM concentration.

Conclusions

The present study provides important information concerning the structural requirements necessary for the recognition of the human A₃ adenosine receptor. It

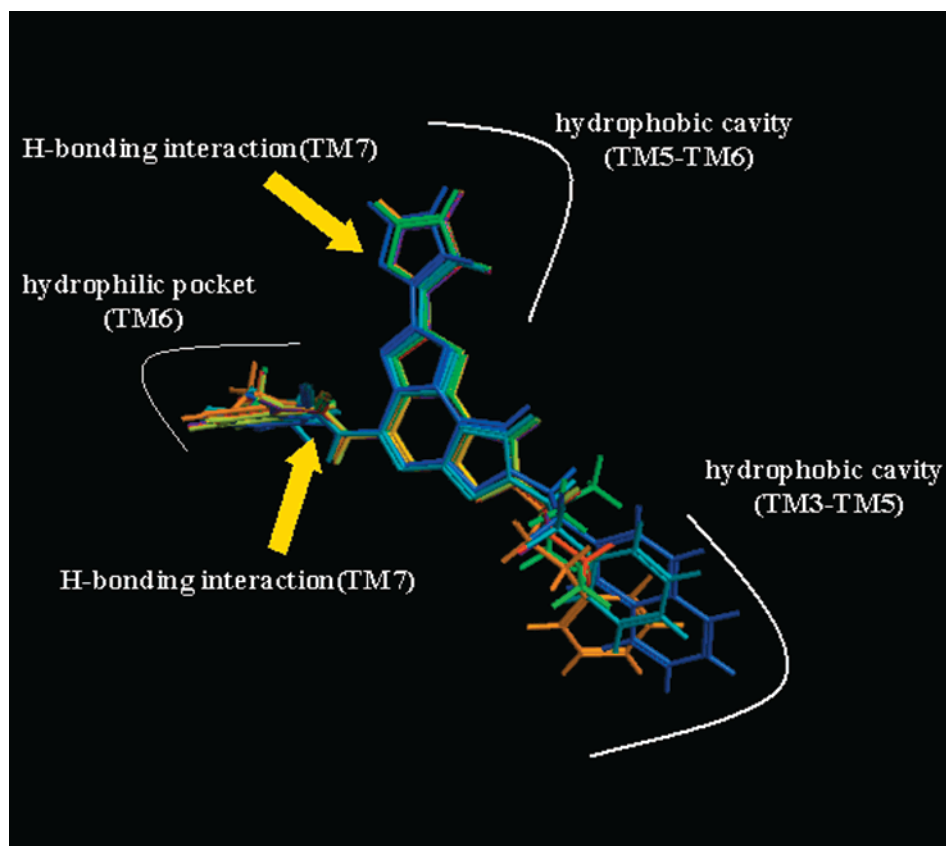


Figure 2. Pharmacophore map for binding at the human A₃ receptor for the tested pyrazolo[4,3-*e*]1,2,4-triazolo[1,5-*c*]pyrimidine derivatives.

Table 3. Functional Assay^a

compd	% inhibition	IC ₅₀ (nM)	compd	% inhibition	IC ₅₀ (nM)	compd	% inhibition	IC ₅₀ (nM)
14	24 (16–35)		23	93 (85–101)	4.1 (2.9–6.0)	11	18 (15–22)	
16	98 (92–105)	1.8 (0.9–3.7)	24	85 (70–103)	4.5 (3.0–6.9)	33	49 (38–63)	
17	88 (77–100)	5.3 (3.8–7.6)	15	9 (5–15)		34	39 (28–55)	
3	26 (14–48)		25	84 (63–110)	6.8 (5.1–8.9)	12	3 (1–9)	
18	94 (79–112)	2.7 (1.7–4.2)	26	70 (62–68)		35	50 (34–73)	
19	92 (81–104)	4.8 (2.8–8.1)	8	14 (8–23)		36	32 (18–59)	
4	25 (15–41)		27	48 (35–65)		13	4 (1–14)	
1	86 (63–116)	4.8 (2.5–9.3)	28	45 (37–54)		37	52 (38–71)	
20	68 (51–91)	14.8 (10.8–21.5)	9	12 (7–19)		38	40 (32–49)	
5	23 (15–35)		29	42 (33–52)		CGS15943	30 (17–52)	406 (354–465)
2	90 (79–106)	5.2 (4.4–6.5)	30	38 (26–54)		39	97 (92–102)	2.0 (1.1–3.8)
21	80 (63–100)	5.5 (4.0–7.5)	10	28 (16–51)		40	95 (84–107)	2.4 (1.8–3.3)
22	90 (73–110)	5.1 (3.5–7.6)	31	78 (64–94)	13.9 (10.7–21.5)			
7	15 (10–21)		32	58 (49–69)				

^a Percentage of blockade by 1 μ M of each compound (**1–40**) of the inhibition by 100 nM IB-MECA-inhibited cAMP accumulation in CHO cells expressing human A₃ adenosine receptors. For the most potent compounds (**1**, **2**, **16–31**, **39**, **40**) and reference compound (CGS15943) IC₅₀ values are also shown. Values are the means of at least three experiments, and in parentheses the 95% confidence limits are shown.

confirms, as previously observed,³⁴ that a substituted phenylcarbamoyl moiety confers affinity and selectivity for the human A₃ adenosine receptor subtype at the pyrazolo[4,3-*e*]1,2,4-triazolo[1,5-*c*]pyrimidine nucleus, while the N⁵ unsubstituted derivatives lacks both affinity and selectivity for human A₃ receptors, showing high affinity for the A₁, A_{2A}, and A_{2B} receptor subtypes. An interesting correlation between the calculated molecular volume of pyrazolo[4,3-*e*]1,2,4-triazolo[1,5-*c*]pyrimidine derivatives and their experimental K_i values has been found. In fact it has been observed that the A₃ affinities decrease with the increasing molecular volume values at the N⁸ position. All these observations suggest that small alkyl groups at the N⁸ pyrazole nitrogen combined with the N⁵-(4-methoxyphenyl)car-

bamoyl substitution afford the best compounds in terms of affinity and selectivity at the human A₃ adenosine receptors. In particular, when the N⁸-methyl and N⁵-(4-methoxyphenyl)carbamoyl substitutions were combined, the most potent and selective human A₃ adenosine antagonist (**18**: hA₃ = 0.2 nM, hA₁/hA₃ = 5485, hA_{2A}/hA₃ = 6950, hA_{2B}/hA₃ = 1305) was obtained.

All these experimental findings were further validated by molecular modeling studies, which demonstrated that bulky substituents at the N⁸ position are not well-tolerated in the pyrazolo[4,3-*e*]1,2,4-triazolo[1,5-*c*]pyrimidine series and that this class of compounds interact perfectly with the human A₃ receptor model proposed by Moro et al.⁴⁵ identifying a possible pharmacophore map.

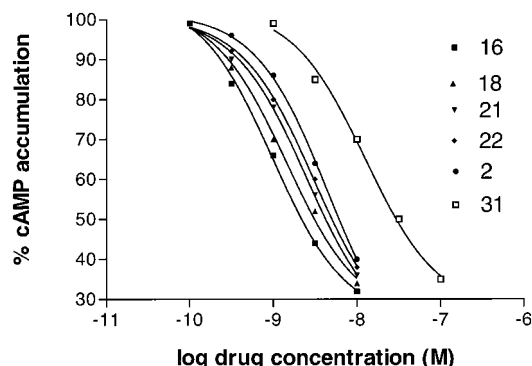


Figure 3. Inhibition curves of cAMP accumulation in human A₃ adenosine receptors by adenosine antagonists blocking the effect of 100 nM IB-MECA. Curves are representative of a single experiment from a series of three independent experiments.

From the results presented herein, it is possible to hypothesize that also the pyrazole nitrogens are indispensable for selectivity at the human A₃ adenosine receptors. In fact, by introducing phenylcarbamoyl moieties on the amino group at the 5-position of CGS15943, retention of affinity but significant loss of selectivity were observed.

Experimental Section

Chemistry. General. Reactions were routinely monitored by thin-layer chromatography (TLC) on silica gel (precoated F₂₅₄ Merck plates) and products visualized with iodine or potassium permanganate solution. Infrared spectra (IR) were measured on a Perkin-Elmer 257 instrument. ¹H NMR were determined in CDCl₃ or DMSO-*d*₆ solutions with a Bruker AC 200 spectrometer, peaks positions are given in parts per million (δ) downfield from tetramethylsilane as internal standard, and *J* values are given in Hz. Light petroleum ether refers to the fractions boiling at 40–60 °C. Melting points were determined on a Buchi-Tottoli instrument and are uncorrected. Chromatographies were performed using Merck 60–200 mesh silica gel. All products reported showed IR and ¹H NMR spectra in agreement with the assigned structures. Organic solutions were dried over anhydrous magnesium sulfate. Elemental analyses were performed by the microanalytical laboratory of Dipartimento di Chimica, University of Ferrara, and were within ±0.4% of the theoretical values for C, H, and N.

Abbreviations: CGS15943, 5-amino-9-chloro-2-(2-furyl)-[1,2,4]triazolo[1,5-*c*]quinazoline; MRS1220, 9-chloro-2-(2-furyl)-[1,2,4]triazolo[1,5-*c*]quinazoline; CHA, *N*⁶-cyclohexyladenosine; DPCPX, 1,3-dipropyl-8-cyclopentylxanthine; DMF, dimethylformamide; DMSO, dimethyl sulfoxide; THF, tetrahydrofuran; CHO cells, Chinese hamster ovary cells; EDTA, ethylenediaminetetraacetate; SCH 58261, 5-amino-2-(2-furyl)-7-(2-phenylethyl)pyrazolo[4,3-*e*][1,2,4]triazolo[1,5-*c*]pyrimidine; IB-MECA, 3-iodobenzyl-5'-(*N*-ethylcarbamoyl)adenosine; NECA, 5'-(*N*-ethylcarbamoyl)adenosine; HEK cells, human embryonic kidney cells; MRE3008-F20, 5-[[4-methoxyphenyl]amino]carbonylamino-8-propyl-2-(2-furyl)pyrazolo[4,3-*e*]1,2,4-triazolo[1,5-*c*]pyrimidine; GTP, guanosine-5'-triphosphate; cAMP, cyclic adenosine-5'-monophosphate; SCH 63390, 5-amino-2-(2-furyl)-7-(3-phenylpropyl)pyrazolo[4,3-*e*][1,2,4]triazolo[1,5-*c*]pyrimidine; TLC, thin-layer chromatography; EtOH, ethanol; mp, melting point; MeOH, methanol; NaH, sodium hydride, EtOAc, ethyl acetate.

General Procedure for Preparation of 8-(Ar)alkyl-2-(2-furyl)pyrazolo[4,3-*e*]1,2,4-triazolo[1,5-*c*]pyrimidines 64–74. A solution of **41** (10 mmol) in 40 mL of DMF cooled to 0 °C was treated with NaH (60% in oil, 12 mmol) in several portions over 10 min. After 45 min, the appropriate (ar)alkyl halide (12 mmol) was added and the reaction mixture was allowed

to warm to 25 °C and stirred for 3–5 h (TLC: EtOAc 1:1). The reaction was quenched by addition of H₂O (80 mL), and the aqueous layer was extracted with EtOAc (5 × 25 mL). The organic layers were recombined, dried (Na₂SO₄), filtered and concentrated at reduced pressure, to afford the alkylated pyrazoles **42–52** as an inseparable mixture of N¹ and N² isomers (ratio approximately 1:4). This mixture of N¹ and N² substituted 4-cyano-5-aminopyrazoles **42–52** was then dissolved in triethyl orthoformate (60 mL) and the solution was refluxed under nitrogen for 8 h. Then the solvent was removed under vacuum, the oily residue constituted by the mixture of imidates **53–63** was dissolved in 2-methoxyethanol (50 mL), and 2-furoic acid hydrazide (13 mmol) was added. The mixture was refluxed for 5–10 h, then, after cooling, the solvent was removed under reduced pressure and the dark oily residue was cyclized further any other purification in diphenyl ether (50 mL) at 260 °C using a Dean–Stark for the azeotropic elimination of water produced in the reaction. After 1.5 h, the mixture was poured onto hexane (300 mL) and cooled. The precipitate was filtered off and purified by chromatography (EtOAc–hexane 1:1). In this way, the major product (N⁸ alkylated) (**64–74**) was obtained in good overall yield.

8-Methyl-2-(2-furyl)pyrazolo[4,3-*e*]1,2,4-triazolo[1,5-*c*]pyrimidine (64). Yield: 45%; yellow solid; mp 155–156 °C (EtOAc–light petroleum). IR (KBr): 1615, 1510 cm⁻¹. ¹H NMR (DMSO-*d*₆): δ 4.1 (s, 3H); 6.32 (m, 1H); 7.25 (m, 1H); 8.06 (m, 1H); 8.86 (s, 1H); 9.38 (s, 1H). Anal. (C₁₁H₈N₆O) C, H, N.

8-Ethyl-2-(2-furyl)pyrazolo[4,3-*e*]1,2,4-triazolo[1,5-*c*]pyrimidine (65). Yield: 50%; pale yellow solid; mp 188–189 °C (EtOAc–light petroleum). IR (KBr): 1620, 1500 cm⁻¹. ¹H NMR (DMSO-*d*₆): δ 1.67 (t, 3H, *J* = 7); 4.53 (q, 2H, *J* = 7); 6.59 (m, 1H); 7.23 (m, 1H); 7.64 (s, 1H); 8.34 (s, 1H); 9.10 (s, 1H). Anal. (C₁₂H₁₀N₆O) C, H, N.

8-Propyl-2-(2-furyl)pyrazolo[4,3-*e*]1,2,4-triazolo[1,5-*c*]pyrimidine (66). Yield: 60%; yellow solid; mp 189–190 °C (EtOAc–light petroleum). IR (KBr): 1600, 1505 cm⁻¹. ¹H NMR (DMSO-*d*₆): δ 0.98 (t, 3H, *J* = 7); 2.03–2.10 (m, 2H); 4.41 (q, 2H, *J* = 7); 6.60 (m, 1H); 7.24 (s, 1H); 7.64 (s, 1H); 8.32 (s, 1H); 9.10 (s, 1H). Anal. (C₁₃H₁₂N₆O) C, H, N.

8-(2-Propen-1-yl)-2-(2-furyl)pyrazolo[4,3-*e*]1,2,4-triazolo[1,5-*c*]pyrimidine (67). Yield: 53%; yellow solid; mp 130–131 °C (EtOAc–light petroleum). IR (KBr): 1620, 1515 cm⁻¹. ¹H NMR (DMSO-*d*₆): δ 4.51–4.54 (m, 1H); 5.04–5.23 (m, 3H); 6.01–6.09 (m, 1H); 6.73 (dd, 1H, *J* = 2, *J* = 4); 7.27 (d, 1H, *J* = 4); 7.96 (d, 1H, *J* = 2); 8.52 (s, 1H); 9.60 (s, 1H). Anal. (C₁₃H₁₀N₆O) C, H, N.

8-*n*-Butyl-2-(2-furyl)pyrazolo[4,3-*e*]1,2,4-triazolo[1,5-*c*]pyrimidine (68). Yield: 50%; pale yellow solid; mp 245–247 °C (EtOAc–light petroleum). IR (KBr): 1610, 1500 cm⁻¹. ¹H NMR (DMSO-*d*₆): δ 0.9 (m, 3H); 1.3 (m, 2H); 1.9 (m, 2H); 4.5 (t, 2H, *J* = 7.2); 6.2 (m, 1H); 7.3 (m, 1H); 8.0 (m, 1H); 8.9 (s, 1H); 9.4 (s, 1H). Anal. (C₁₄H₁₄N₆O) C, H, N.

8-(3-Methyl-1-butyl)-2-(2-furyl)pyrazolo[4,3-*e*]1,2,4-triazolo[1,5-*c*]pyrimidine (69). Yield: 54%; pale yellow solid; mp 235–237 °C (EtOAc–light petroleum). IR (KBr): 1635, 1510, 1450 cm⁻¹. ¹H NMR (DMSO-*d*₆): δ 1.0 (d, 6H, *J* = 6.2); 1.5–1.9 (m, 3H); 4.6 (t, 2H, *J* = 7.4); 6.6 (m, 1H); 7.3 (m, 1H); 7.7 (m, 1H); 8.8 (s, 1H); 9.1 (s, 1H). Anal. (C₁₅H₁₆N₆O) C, H, N.

8-(3-Methyl-2-buten-1-yl)-2-(2-furyl)pyrazolo[4,3-*e*]1,2,4-triazolo[1,5-*c*]pyrimidine (70). Yield: 48%; yellow solid; mp 210–212 °C (EtOAc–light petroleum). IR (KBr): 1625, 1500, 1430 cm⁻¹. ¹H NMR (DMSO-*d*₆): δ 1.79 (s, 3H); 1.87 (s, 3H); 5.05 (d, 2H, *J* = 6); 5.55–5.63 (m, 1H); 6.60 (m, 1H); 7.24 (m, 1H); 7.64 (s, 1H); 8.34 (s, 1H); 9.10 (s, 1H). Anal. (C₁₅H₁₄N₆O) C, H, N.

8-(2-Phenylethyl)-2-(2-furyl)pyrazolo[4,3-*e*]1,2,4-triazolo[1,5-*c*]pyrimidine (71). Yield: 56%; yellow solid; mp 268–270 °C (EtOAc–light petroleum). IR (KBr): 1660, 1510, 1450 cm⁻¹. ¹H NMR (DMSO-*d*₆): δ 3.32 (t, 2H, *J* = 6.7); 4.72 (t, 2H, *J* = 6.7); 6.73 (s, 1H); 7.23 (m, 5H); 7.95 (s, 1H); 8.8 (s, 1H); 9.41 (s, 1H). Anal. (C₁₈H₁₄N₆O) C, H, N.

8-(3-Phenylpropyl)-2-(2-furyl)pyrazolo[4,3-*e*]1,2,4-triazolo[1,5-*c*]pyrimidine (72). Yield: 63%; yellow solid; mp

165–166 °C (EtOAc–light petroleum). IR (KBr): 1630, 1500, 1440 cm^{-1} . ^1H NMR (DMSO- d_6): δ 2.34–2.48 (m, 2H); 2.67 (t, 2H, $J = 7.5$); 4.43 (t, 2H, $J = 7.5$); 6.61 (m, 1H); 7.16–7.32 (m, 6H); 7.64 (d, 1H, $J = 2$); 8.29 (s, 1H); 9.02 (s, 1H). Anal. ($\text{C}_{19}\text{H}_{16}\text{N}_6\text{O}$) C, H, N.

8-[2-(2',4',5'-Tribromophenyl)ethyl]-2-(2-furyl)pyrazolo[4,3-*e*]1,2,4-triazolo[1,5-*c*]pyrimidine (73). Yield: 49%; yellow solid; mp 215–218 °C (EtOAc–light petroleum). IR (KBr): 1650, 1520, 1455 cm^{-1} . ^1H NMR (DMSO- d_6): δ 3.39 (t, 2H, $J = 6.7$); 4.79 (t, 2H, $J = 6.7$); 6.73–6.75 (m, 1H); 7.03 (s, 1H); 7.27 (d, 1H, $J = 4$); 7.42 (s, 1H); 7.91 (d, 1H, $J = 2$); 8.45 (s, 1H); 9.31 (s, 1H). Anal. ($\text{C}_{18}\text{H}_{11}\text{N}_6\text{OBr}_3$) C, H, N.

8-[2-(α -Naphthyl)ethyl]-2-(2-furyl)pyrazolo[4,3-*e*]1,2,4-triazolo[1,5-*c*]pyrimidine (74). Yield: 53%; yellow solid; mp 182–183 °C (EtOAc–light petroleum). IR (KBr): 1635, 1515, 1450 cm^{-1} . ^1H NMR (DMSO- d_6): δ 3.31 (t, 2H, $J = 6.7$); 4.53 (t, 2H, $J = 6.7$); 6.61 (dd, 1H, $J = 2$, $J = 4$); 7.23–7.48 (m, 5H); 7.53–7.73 (m, 3H); 7.83 (d, 1H, $J = 2$); 8.45 (s, 1H); 9.27 (s, 1H). Anal. ($\text{C}_{22}\text{H}_{16}\text{N}_6\text{O}$) C, H, N.

General Procedure for Preparation of 5-Amino-8-(ar)-alkyl-2-(2-furyl)pyrazolo[4,3-*e*]1,2,4-triazolo[1,5-*c*]pyrimidines 3–13. A solution of the mixture of triazolo pyrimidine **64–74** (10 mmol) in aqueous 10% HCl (50 mL) was refluxed for 3 h. Then the solution was cooled and neutralized with a saturated solution of NaHCO_3 at 0 °C. The compounds **75–85** were extracted with EtOAc (3 \times 20 mL); the organic layers were dried with Na_2SO_4 and evaporated under vacuum. The obtained crude amine **75–85** was dissolved in *N*-methylpyrrolidone (40 mL), cyanamide (60 mmol) and *p*-toluenesulfonic acid (15 mmol) were added, and the mixture was heated at 160 °C for 4 h. Then cyanamide (60 mmol) was added again, and the solution was heated overnight. Then the solution was diluted with EtOAc (80 mL), and the precipitate (excess of cyanamide) was filtered off; the filtrate was concentrated under reduced pressure and washed with water (3 \times 30 mL). The organic layer was dried (Na_2SO_4) and evaporated under vacuum. The residue was purified by flash chromatography (EtOAc–light petroleum 2:1) to afford the desired product (**3–13**) as a solid.

5-Amino-8-methyl-2-(2-furyl)pyrazolo[4,3-*e*]1,2,4-triazolo[1,5-*c*]pyrimidine (3). Yield: 53%; yellow solid. IR (KBr): 3500–2950, 1680, 1645, 1610, 1560, 1455 cm^{-1} . ^1H NMR (DMSO- d_6): δ 4.12 (s, 3H); 6.70 (m, 1H); 6.99 (bs, 2H); 7.18 (m, 1H); 7.81 (s, 1H); 8.42 (s, 1H).

5-Amino-8-ethyl-2-(2-furyl)pyrazolo[4,3-*e*]1,2,4-triazolo[1,5-*c*]pyrimidine (4). Yield: 65%; yellow solid. IR (KBr): 3430–2950, 1680, 1655, 1620, 1550, 1450 cm^{-1} . ^1H NMR (DMSO- d_6): δ 1.46 (t, 3H, $J = 7$); 4.30 (d, 2H, $J = 7$); 6.72 (m, 1H); 7.18 (m, 1H); 7.93 (bs, 2H); 7.93 (s, 1H); 8.62 (s, 1H).

5-Amino-8-propyl-2-(2-furyl)pyrazolo[4,3-*e*]1,2,4-triazolo[1,5-*c*]pyrimidine (5). Yield: 57%; pale yellow solid. IR (KBr): 3400–2900, 1660, 1645, 1610, 1545, 1430 cm^{-1} . ^1H NMR (DMSO- d_6): δ 0.83 (t, 3H, $J = 7$); 1.81–1.91 (m, 2H); 4.22 (d, 2H, $J = 7$); 6.71 (m, 1H); 7.19 (m, 1H); 7.63 (bs, 2H); 7.93 (s, 1H); 8.61 (s, 1H).

5-Amino-8-(2-propen-1-yl)-2-(2-furyl)pyrazolo[4,3-*e*]1,2,4-triazolo[1,5-*c*]pyrimidine (6). Yield: 48%; yellow solid. IR (KBr): 3350–2970, 1625, 1510 cm^{-1} . ^1H NMR (DMSO- d_6): δ 4.93 (d, 2H, $J = 6$); 5.33–5.42 (m, 2H); 6.01–6.09 (m, 1H); 6.47 (bs, 1H); 6.58 (dd, 1H, $J = 2$, $J = 4$); 7.20 (d, 1H, $J = 4$); 7.62 (d, 1H, $J = 2$); 8.17 (s, 1H).

5-Amino-8-*n*-butyl-2-(2-furyl)pyrazolo[4,3-*e*]1,2,4-triazolo[1,5-*c*]pyrimidine (7). Yield: 47%; white solid. IR (KBr): 3500–2900, 1685, 1640, 1620, 1550, 1450 cm^{-1} . ^1H NMR (DMSO- d_6): δ 0.9 (t, 3H); 1.2 (m, 2H); 1.8 (m, 2H); 4.2 (t, 2H); 6.7 (m, 1H); 7.2 (m, 2H); 7.6 (s, 1H); 8.0 (s, 1H); 8.6 (s, 1H).

5-Amino-8-(3-methyl-1-butyl)-2-(2-furyl)pyrazolo[4,3-*e*]1,2,4-triazolo[1,5-*c*]pyrimidine (8). Yield: 60%; off-white solid. IR (KBr): 3500–2850, 1670, 1650, 1615, 1560, 1455 cm^{-1} . ^1H NMR (DMSO- d_6): δ 0.96 (d, 6H, $J = 6.4$); 1.59 (m, 1H); 1.86 (m, 2H); 4.32 (t, 2H, $J = 6.4$); 6.58 (m, 1H); 6.72 (bs, 2H); 7.21 (d, 1H, $J = 4.2$); 7.63 (d, 1H, $J = 1.2$); 8.10 (s, 1H).

5-Amino-8-(3-methyl-2-buten-1-yl)-2-(2-furyl)pyrazolo[4,3-*e*]1,2,4-triazolo[1,5-*c*]pyrimidine (9). Yield: 58%; pale yellow solid. IR (KBr): 3520–2950, 1665, 1640, 1610, 1555, 1450 cm^{-1} . ^1H NMR (DMSO- d_6): δ 1.74 (s, 3H); 1.77 (s, 3H); 4.87 (d, 2H, $J = 7$); 5.43–5.46 (m, 1H); 6.72 (m, 1H); 7.18 (m, 1H); 7.62 (bs, 2H); 7.93 (s, 1H); 8.55 (s, 1H).

5-Amino-8-(2-phenylethyl)-2-(2-furyl)pyrazolo[4,3-*e*]1,2,4-triazolo[1,5-*c*]pyrimidine (10). Yield: 45%; white solid. IR (KBr): 3500–2900, 1670, 1645, 1620, 1530, 1455 cm^{-1} . ^1H NMR (DMSO- d_6): δ 3.21 (t, 2H, $J = 6.4$); 4.53 (t, 2H, $J = 6.4$); 6.7 (s, 1H); 7.1–7.4 (m, 6H); 7.65 (bs, 2H); 7.93 (s, 1H); 8.45 (s, 1H).

5-Amino-8-(3-phenylpropyl)-2-(2-furyl)pyrazolo[4,3-*e*]1,2,4-triazolo[1,5-*c*]pyrimidine (11). Yield: 57%; yellow solid. IR (KBr): 3510–2950, 1665, 1640, 1615, 1520, 1455 cm^{-1} . ^1H NMR (DMSO- d_6): δ 2.14–2.21 (m, 2H); 2.54 (t, 2H, $J = 7$); 4.29 (t, 2H, $J = 6.4$); 6.72 (s, 1H); 7.14–7.32 (m, 6H); 7.64 (bs, 2H); 7.93 (s, 1H); 8.64 (s, 1H).

5-Amino-8-[2-(2',4',5'-tribromophenyl)ethyl]-2-(2-furyl)pyrazolo[4,3-*e*]1,2,4-triazolo[1,5-*c*]pyrimidine (12). Yield: 49%; yellow solid. IR (KBr): 3300–2900, 1655, 1520, 1455 cm^{-1} . ^1H NMR (DMSO- d_6): δ 3.41 (t, 2H, $J = 6.7$); 4.73 (t, 2H, $J = 6.7$); 6.70–6.75 (m, 1H); 7.10 (s, 1H); 7.25 (d, 1H, $J = 4$); 7.38 (s, 1H); 7.65 (bs, 2H); 7.87 (d, 1H, $J = 2$); 8.25 (s, 1H).

5-Amino-8-[2-(α -naphthyl)ethyl]-2-(2-furyl)pyrazolo[4,3-*e*]1,2,4-triazolo[1,5-*c*]pyrimidine (13). Yield: 53%; yellow solid. IR (KBr): 3345–2980, 1630, 1520, 1450 cm^{-1} . ^1H NMR (DMSO- d_6): δ 3.37 (t, 2H, $J = 6.5$); 4.41 (t, 2H, $J = 6.5$); 6.65 (dd, 1H, $J = 2$, $J = 4$); 7.33–7.51 (m, 5H); 7.61 (bs, 2H); 7.65–7.73 (m, 3H); 7.87 (d, 1H, $J = 2$); 8.23 (s, 1H).

Preparation of 5-Amino-2-(2-furyl)pyrazolo[4,3-*e*]1,2,4-triazolo[1,5-*c*]pyrimidine (14) and 5-Amino-8-*tert*-butyl-2-(2-furyl)pyrazolo[4,3-*e*]1,2,4-triazolo[1,5-*c*]pyrimidine (15). A solution of **86** (297 mg, 1 mmol) in formic acid 98% (15 mL) was heated at 130 °C for 48 h. Then the solvent was removed at reduced pressure and the residue purified by chromatography (EtOAc–MeOH 7:3) to afford **14** and **15**, respectively, as yellow solids.

14: yield 43%; yellow solid. IR (KBr): 3345–2990, 1620, 1515, 1450 cm^{-1} . ^1H NMR (DMSO- d_6): δ 6.71 (dd, 1H, $J = 2$, $J = 4$); 7.22 (d, 1H, $J = 4$); 7.92 (d, 1H, $J = 2$); 7.98 (bs, 2H); 8.17 (s, 1H); 11.34 (bs, 1H).

15: yield 38%; pale yellow solid. IR (KBr): 3350–2950, 1615, 1520, 1450 cm^{-1} . ^1H NMR (DMSO- d_6): δ 1.61 (s, 9H); 6.72 (dd, 1H, $J = 2$, $J = 4$); 7.16 (d, 1H, $J = 4$); 7.59 (bs, 2H); 7.93 (d, 1H, $J = 2$); 8.78 (s, 1H).

General Procedure for Preparation of 5-[[Substituted-phenyl]amino]carbonylamino-8-(ar)alkyl-2-(2-furyl)pyrazolo[4,3-*e*]1,2,4-triazolo[1,5-*c*]pyrimidines 1, 2, and 16–38 and 5-[[Substituted-phenyl]amino]carbonylamino-9-chloro-2-(2-furyl)[1,2,4]triazolo[1,5-*c*]quinazolines 39 and 40. Amino compound **3–13** (CGS15943) (10 mmol) was dissolved in freshly distilled THF (15 mL) and the appropriate isocyanate (**87**, **88**) (13 mmol) was added. The mixture was refluxed under argon for 18 h. Then the solvent was removed under reduced pressure and the residue was purified by flash chromatography (EtOAc–light petroleum 4:6) to afford the desired compounds **1**, **2**, and **16–40**.

5-[[4-Methoxyphenyl]amino]carbonylamino-2-(2-furyl)pyrazolo[4,3-*e*]1,2,4-triazolo[1,5-*c*]pyrimidine (16). Yield: 84%; pale yellow solid. IR (KBr): 3245–2980, 1685, 1615, 1520, 1450 cm^{-1} . ^1H NMR (DMSO- d_6): δ 3.78 (s, 3H); 6.54 (dd, 2H, $J = 2$, $J = 4$); 7.35 (d, 1H, $J = 4$); 7.50 (d, 2H, $J = 9$); 7.83 (d, 2H, $J = 9$); 8.01 (d, 1H, $J = 2$); 8.03 (s, 1H); 9.45 (bs, 1H); 10.81 (bs, 1H); 11.09 (bs, 1H).

5-[[3-Chlorophenyl]amino]carbonylamino-2-(2-furyl)pyrazolo[4,3-*e*]1,2,4-triazolo[1,5-*c*]pyrimidine (17). Yield: 78%; pale yellow solid. IR (KBr): 3240–2980, 1680, 1625, 1530, 1435 cm^{-1} . ^1H NMR (DMSO- d_6): δ 6.80 (dd, 2H, $J = 2$, $J = 4$); 7.26–7.45 (m, 4H); 7.75–8.02 (m, 3H); 8.35 (s, 1H); 9.48 (bs, 1H); 11.11 (bs, 1H); 11.42 (bs, 1H).

5-[[4-Methoxyphenyl]amino]carbonylamino-8-methyl-2-(2-furyl)pyrazolo[4,3-*e*]1,2,4-triazolo[1,5-*c*]pyrimi-

dine (18). Yield: 99%; yellow solid. IR (KBr): 3200–2900, 1664, 1625, 1600, 1500 cm^{-1} . ^1H NMR (CDCl_3): δ 3.81 (s, 3H); 4.20 (s, 3H); 6.61 (m, 1H); 6.85 (d, 2H, $J = 9$); 7.26 (m, 1H); 7.55 (d, 2H, $J = 9$); 7.65 (s, 1H); 8.21 (s, 1H); 8.59 (bs, 1H); 10.96 (bs, 1H).

5-[(3-Chlorophenyl)amino]carbonylamino-8-methyl-2-(2-furyl)pyrazolo[4,3-*e*]1,2,4-triazolo[1,5-*c*]pyrimidine (19). Yield: 98%; pale yellow solid. IR (KBr): 3210–2930, 1660, 1630, 1610, 1500 cm^{-1} . ^1H NMR (CDCl_3): δ 4.21 (s, 3H); 6.60 (m, 1H); 7.11 (d, 1H, $J = 8$); 7.13–7.28 (m, 2H); 7.55 (d, 1H, $J = 8$); 7.65 (s, 1H); 7.78 (d, 1H, $J = 2$); 8.22 (s, 1H); 8.61 (bs, 1H); 11.24 (bs, 1H).

5-[(4-Methoxyphenyl)amino]carbonylamino-8-ethyl-2-(2-furyl)pyrazolo[4,3-*e*]1,2,4-triazolo[1,5-*c*]pyrimidine (1). Yield: 99%; pale yellow solid. IR (KBr): 3250–2950, 1665, 1620, 1610, 1520 cm^{-1} . ^1H NMR (CDCl_3): δ 1.71 (t, 3H, $J = 7$); 3.85 (s, 3H); 4.49 (q, 2H, $J = 7$); 6.65 (m, 1H); 6.88 (d, 2H, $J = 9$); 7.26 (m, 1H); 7.58 (d, 2H, $J = 9$); 7.69 (s, 1H); 8.28 (s, 1H); 8.63 (bs, 1H); 10.99 (bs, 1H).

5-[(3-Chlorophenyl)amino]carbonylamino-8-ethyl-2-(2-furyl)pyrazolo[4,3-*e*]1,2,4-triazolo[1,5-*c*]pyrimidine (20). Yield: 98%; pale yellow solid. IR (KBr): 3220–2930, 1660, 1620, 1600, 1500 cm^{-1} . ^1H NMR (CDCl_3): δ 1.71 (t, 3H, $J = 7$); 4.50 (q, 2H, $J = 7$); 6.67 (m, 1H); 7.20 (d, 1H, $J = 8$); 7.31 (m, 1H); 7.61 (d, 1H, $J = 8$); 7.70 (s, 1H); 7.84 (s, 1H); 8.30 (s, 1H); 8.67 (bs, 1H); 11.30 (bs, 1H).

5-[(4-Methoxyphenyl)amino]carbonylamino-8-propyl-2-(2-furyl)pyrazolo[4,3-*e*]1,2,4-triazolo[1,5-*c*]pyrimidine (2). Yield: 98%; pale yellow solid. IR (KBr): 3230–2950, 1660, 1620, 1600, 1530 cm^{-1} . ^1H NMR (CDCl_3): δ 0.98 (t, 3H, $J = 7$); 2.04–2.08 (m, 2H); 3.82 (s, 3H); 4.35 (t, 2H, $J = 7$); 6.61 (m, 1H); 6.89 (d, 2H, $J = 9$); 7.25 (m, 1H); 7.56 (d, 2H, $J = 9$); 7.65 (s, 1H); 8.23 (s, 1H); 8.59 (bs, 1H); 10.95 (bs, 1H).

5-[(3-Chlorophenyl)amino]carbonylamino-8-propyl-2-(2-furyl)pyrazolo[4,3-*e*]1,2,4-triazolo[1,5-*c*]pyrimidine (21). Yield: 95%; white solid. IR (KBr): 3210–2920, 1655, 1615, 1600, 1510 cm^{-1} . ^1H NMR (CDCl_3): δ 1.71 (t, 3H, $J = 7$); 2.04 (m, 2H); 4.36 (q, 2H, $J = 7$); 6.62 (m, 1H); 7.12 (d, 1H, $J = 8$); 7.27 (m, 1H); 7.56 (d, 1H, $J = 8$); 7.66 (s, 1H); 7.80 (s, 1H); 8.24 (s, 1H); 8.62 (bs, 1H); 11.08 (bs, 1H).

5-[(4-Methoxyphenyl)amino]carbonylamino-8-(2-propen-1-yl)-2-(2-furyl)pyrazolo[4,3-*e*]1,2,4-triazolo[1,5-*c*]pyrimidine (22). Yield: 90%; white solid. IR (KBr): 3210–2920, 1665, 1620, 1600, 1520 cm^{-1} . ^1H NMR (CDCl_3): δ 3.83 (s, 3H); 5.01 (d, 2H, $J = 7$); 5.36–5.48 (m, 2H); 6.03–6.16 (m, 1H); 6.62 (dd, 1H, $J = 2$, $J = 4$); 6.91 (d, 2H, $J = 9$); 7.25 (d, 1H, $J = 4$); 7.56 (d, 1H, $J = 9$); 7.67 (d, 1H, $J = 2$); 8.28 (s, 1H); 8.65 (bs, 1H); 10.94 (bs, 1H).

5-[(4-Methoxyphenyl)amino]carbonylamino-8-*n*-butyl-2-(2-furyl)pyrazolo[4,3-*e*]1,2,4-triazolo[1,5-*c*]pyrimidine (23). Yield: 96%; white solid. IR (KBr): 3250–2960, 1665, 1610, 1600, 1520 cm^{-1} . ^1H NMR (CDCl_3): δ 0.98 (t, 3H, $J = 7$); 1.38–1.42 (m, 2H); 2.02–2.05 (m, 2H); 3.82 (s, 3H); 4.39 (t, 2H, $J = 7$); 6.63 (m, 1H); 6.92 (d, 2H, $J = 9$); 7.25 (m, 1H); 7.57 (d, 2H, $J = 9$); 7.67 (s, 1H); 8.23 (s, 1H); 8.60 (bs, 1H); 10.95 (bs, 1H).

5-[(3-Chlorophenyl)amino]carbonylamino-8-*n*-butyl-2-(2-furyl)pyrazolo[4,3-*e*]1,2,4-triazolo[1,5-*c*]pyrimidine (24). Yield: 97%; white solid. IR (KBr): 3240–2970, 1650, 1610, 1510 cm^{-1} . ^1H NMR (CDCl_3): δ 1.00 (t, 3H, $J = 7$); 1.39–1.41 (m, 2H); 1.99–2.03 (m, 2H); 4.41 (q, 2H, $J = 7$); 6.63 (m, 1H); 7.14 (d, 1H, $J = 8$); 7.29 (m, 1H); 7.56 (d, 1H, $J = 8$); 7.67 (s, 1H); 7.80 (s, 1H); 8.25 (s, 1H); 8.63 (bs, 1H); 11.26 (bs, 1H).

5-[(4-Methoxyphenyl)amino]carbonylamino-8-*tert*-butyl-2-(2-furyl)pyrazolo[4,3-*e*]1,2,4-triazolo[1,5-*c*]pyrimidine (25). Yield: 97%; white solid. IR (KBr): 3220–2990, 1658, 1615, 1512 cm^{-1} . ^1H NMR (CDCl_3): δ 1.75 (s, 9H); 3.81 (s, 3H); 6.59 (dd, 1H, $J = 2$, $J = 4$); 6.90 (d, 2H, $J = 8$); 7.24 (d, 1H, $J = 4$); 7.55 (d, 2H, $J = 9$); 7.64 (d, 1H, $J = 2$); 8.37 (s, 1H); 8.59 (bs, 1H); 10.93 (bs, 1H).

5-[(3-Chlorophenyl)amino]carbonylamino-8-*tert*-butyl-2-(2-furyl)pyrazolo[4,3-*e*]1,2,4-triazolo[1,5-*c*]pyrimidine (26). Yield: 93%; white solid. IR (KBr): 3220–2950, 1665, 1620, 1500 cm^{-1} . ^1H NMR (CDCl_3): δ 1.76 (s, 9H); 6.60

(dd, 1H, $J = 2$, $J = 4$); 7.14–7.34 (m, 3H); 7.55–7.64 (m, 2H); 7.82 (d, 1H, $J = 2$); 8.39 (s, 1H); 8.62 (bs, 1H); 11.25 (bs, 1H).

5-[(4-Methoxyphenyl)amino]carbonylamino-8-(3-methyl-1-butyl)-2-(2-furyl)pyrazolo[4,3-*e*]1,2,4-triazolo[1,5-*c*]pyrimidine (27). Yield: 98%; white solid. IR (KBr): 3230–2970, 1660, 1615, 1600, 1500 cm^{-1} . ^1H NMR (CDCl_3): δ 0.99 (d, 6H, $J = 7.5$); 1.58–1.22 (m, 1H); 1.87–1.97 (m, 2H); 3.82 (s, 3H); 4.40 (t, 2H, $J = 7$); 6.62 (m, 1H); 6.91 (d, 2H, $J = 9$); 7.23 (m, 1H); 7.58 (d, 2H, $J = 9$); 7.66 (s, 1H); 8.23 (s, 1H); 8.59 (bs, 1H); 10.94 (bs, 1H).

5-[(3-Chlorophenyl)amino]carbonylamino-8-(3-methyl-1-butyl)-2-(2-furyl)pyrazolo[4,3-*e*]1,2,4-triazolo[1,5-*c*]pyrimidine (28). Yield: 97%; pale yellow solid. IR (KBr): 3230–2950, 1655, 1600, 1510 cm^{-1} . ^1H NMR (CDCl_3): δ 1.01 (d, 6H, $J = 7.5$); 1.49–1.51 (m, 1H); 1.88–2.03 (m, 2H); 4.42 (t, 2H, $J = 7$); 6.62 (m, 1H); 7.13 (d, 1H, $J = 8$); 7.34 (m, 1H); 7.57 (d, 1H, $J = 8$); 7.67 (s, 1H); 7.80 (s, 1H); 8.24 (s, 1H); 8.63 (bs, 1H); 11.25 (bs, 1H).

5-[(4-Methoxyphenyl)amino]carbonylamino-8-(3-methyl-2-buten-1-yl)-2-(2-furyl)pyrazolo[4,3-*e*]1,2,4-triazolo[1,5-*c*]pyrimidine (29). Yield: 96%; pale yellow solid. IR (KBr): 3235–2950, 1665, 1620, 1600, 1510 cm^{-1} . ^1H NMR (CDCl_3): δ 1.83 (s, 3H); 1.87 (s, 3H); 3.81 (s, 3H); 4.97 (d, 2H, $J = 7$); 5.57 (m, 1H); 6.61 (m, 1H); 6.93 (d, 2H, $J = 9$); 7.24 (m, 1H); 7.54 (d, 2H, $J = 9$); 7.66 (s, 1H); 8.25 (s, 1H); 8.58 (bs, 1H); 10.96 (bs, 1H).

5-[(3-Chlorophenyl)amino]carbonylamino-8-(3-methyl-2-buten-1-yl)-2-(2-furyl)pyrazolo[4,3-*e*]1,2,4-triazolo[1,5-*c*]pyrimidine (30). Yield: 99%; white solid. IR (KBr): 3245–2960, 1650, 1600, 1510 cm^{-1} . ^1H NMR (CDCl_3): δ 1.84 (s, 3H); 1.88 (s, 3H); 5.01 (d, 2H, $J = 8$); 5.57 (m, 1H); 6.62 (m, 1H); 7.12 (d, 1H, $J = 8$); 7.29 (m, 1H); 7.56 (d, 1H, $J = 8$); 7.66 (s, 1H); 7.80 (s, 1H); 8.26 (s, 1H); 8.60 (bs, 1H); 11.26 (bs, 1H).

5-[(4-Methoxyphenyl)amino]carbonylamino-8-(2-phenylethyl)-2-(2-furyl)pyrazolo[4,3-*e*]1,2,4-triazolo[1,5-*c*]pyrimidine (31). Yield: 99%; white solid. IR (KBr): 3245–2960, 1660, 1615, 1600, 1500 cm^{-1} . ^1H NMR (CDCl_3): δ 3.42 (t, 2H, $J = 7$); 3.82 (s, 3H); 4.60 (t, 2H, $J = 7$); 6.60 (m, 1H); 6.93 (d, 2H, $J = 9$); 7.09 (m, 2H); 7.20–7.28 (m, 4H); 7.56 (d, 2H, $J = 8$); 7.60 (s, 1H); 7.89 (s, 1H); 8.59 (bs, 1H); 10.96 (bs, 1H).

5-[(3-Chlorophenyl)amino]carbonylamino-8-(2-phenylethyl)-2-(2-furyl)pyrazolo[4,3-*e*]1,2,4-triazolo[1,5-*c*]pyrimidine (32). Yield: 98%; white solid. IR (KBr): 3250–2970, 1660, 1610, 1515 cm^{-1} . ^1H NMR (CDCl_3): δ 3.33 (t, 2H, $J = 7$); 4.62 (t, 2H, $J = 7$); 6.60 (m, 1H); 7.19–7.35 (m, 7H); 7.57 (d, 1H, $J = 8$); 7.61 (s, 1H); 7.81 (s, 1H); 7.89 (s, 1H); 8.63 (bs, 1H); 11.27 (bs, 1H).

5-[(4-Methoxyphenyl)amino]carbonylamino-8-(3-phenylpropyl)-2-(2-furyl)pyrazolo[4,3-*e*]1,2,4-triazolo[1,5-*c*]pyrimidine (33). Yield: 98%; white solid. IR (KBr): 3240–2950, 1665, 1615, 1600, 1510 cm^{-1} . ^1H NMR (CDCl_3): δ 2.46 (m, 2H); 2.73 (t, 2H, $J = 7$); 4.42 (t, 2H, $J = 7$); 6.67 (m, 1H); 6.96 (d, 2H, $J = 9$); 7.22–7.41 (m, 6H); 7.60 (d, 2H, $J = 8$); 7.64 (s, 1H); 8.25 (s, 1H); 8.65 (bs, 1H); 11.16 (bs, 1H).

5-[(3-Chlorophenyl)amino]carbonylamino-8-(3-phenylpropyl)-2-(2-furyl)pyrazolo[4,3-*e*]1,2,4-triazolo[1,5-*c*]pyrimidine (34). Yield: 99%; pale yellow solid. IR (KBr): 3245–2960, 1665, 1610, 1515 cm^{-1} . ^1H NMR (CDCl_3): δ 2.46 (m, 2H); 2.73 (t, 2H, $J = 7$); 4.43 (t, 2H, $J = 7$); 6.66 (m, 1H); 7.19–7.40 (m, 8H); 7.59 (d, 1H, $J = 8$); 7.64 (s, 1H); 7.85 (m, 1H); 8.25 (s, 1H); 8.67 (bs, 1H); 11.30 (bs, 1H).

5-[(4-Methoxyphenyl)amino]carbonylamino-8-[2-(2',4',5'-tribromophenyl)ethyl]-2-(2-furyl)pyrazolo[4,3-*e*]1,2,4-triazolo[1,5-*c*]pyrimidine (35). Yield: 79%; yellow solid. IR (KBr): 3230–2960, 1665, 1615, 1600, 1500 cm^{-1} . ^1H NMR (CDCl_3): δ 3.39 (t, 2H, $J = 7$); 3.80 (s, 3H); 4.57 (t, 2H, $J = 7$); 6.63 (dd, 1H, $J = 2$, $J = 4$); 7.09 (s, 1H); 7.27 (d, 1H, $J = 4$); 7.43 (s, 1H); 7.62 (d, 1H, $J = 2$); 8.01 (s, 1H); 8.63 (bs, 1H); 11.11 (bs, 1H).

5-[(3-Chlorophenyl)amino]carbonylamino-8-[2-(2',4',5'-tribromophenyl)ethyl]-2-(2-furyl)pyrazolo[4,3-*e*]1,2,4-triazolo[1,5-*c*]pyrimidine (36). Yield: 83%; yellow solid. IR (KBr): 3250–2930, 1670, 1620, 1600, 1500 cm^{-1} . ^1H NMR (CDCl_3): δ 3.41 (t, 2H, $J = 7$); 4.63 (t, 2H, $J = 7$); 6.63 (dd,

1H, $J = 2$, $J = 4$); 7.05–7.48 (m, 5H); 7.51–7.78 (m, 3H); 8.06 (s, 1H); 8.65 (bs, 1H); 11.25 (bs, 1H).

5-[[[(4-Methoxyphenyl)amino]carbonyl]amino-8-[2-(α -naphthyl)ethyl]-2-(2-furyl)pyrazolo[4,3-*e*]1,2,4-triazolo[1,5-*c*]pyrimidine (37). Yield: 68%; yellow solid. IR (KBr): 3285–2970, 1665, 1610, 1520, 1450 cm^{-1} . ^1H NMR (CDCl_3): δ 3.35 (t, 2H, $J = 6.5$); 3.84 (s, 3H); 4.41 (t, 2H, $J = 6.5$); 6.63 (dd, 1H, $J = 2$, $J = 4$); 7.19–7.55 (m, 7H); 7.61–7.90 (m, 6H); 8.05 (s, 1H); 8.97 (bs, 1H); 10.57 (bs, 1H).

5-[[[(3-Chlorophenyl)amino]carbonyl]amino-8-[2-(α -naphthyl)ethyl]-2-(2-furyl)pyrazolo[4,3-*e*]1,2,4-triazolo[1,5-*c*]pyrimidine (38). Yield: 68%; yellow solid. IR (KBr): 3300–2975, 1660, 1615, 1515, 1450 cm^{-1} . ^1H NMR (CDCl_3): δ 3.37 (t, 2H, $J = 6.5$); 4.38 (t, 2H, $J = 6.5$); 6.62 (dd, 1H, $J = 2$, $J = 4$); 7.08–7.46 (m, 7H); 7.57–7.89 (m, 6H); 8.02 (s, 1H); 9.45 (bs, 1H); 11.34 (bs, 1H).

5-[[[(4-Methoxyphenyl)amino]carbonyl]amino-9-chloro-2-(2-furyl)[1,2,4]triazolo[1,5-*c*]quinazoline (39). Yield: 88%; pale yellow solid. IR (KBr): 3250–2975, 1665, 1610, 1515, 1450 cm^{-1} . ^1H NMR (CDCl_3): δ 3.80 (s, 3H); 6.65 (dd, 1H, $J = 2$, $J = 4$); 6.87 (d, 1H, $J = 8$); 6.95 (d, 2H, $J = 11$); 7.27 (d, 2H, $J = 11$); 7.53 (d, 1H, $J = 4$); 7.56 (d, 1H, $J = 8$); 7.70 (d, 1H, $J = 2$); 7.79 (s, 1H); 8.53 (bs, 1H); 11.18 (bs, 1H).

5-[[[(3-Chlorophenyl)amino]carbonyl]amino-9-chloro-2-(2-furyl)[1,2,4]triazolo[1,5-*c*]quinazoline (40). Yield: 92%; pale yellow solid. IR (KBr): 3280–2955, 1668, 1615, 1510, 1450 cm^{-1} . ^1H NMR (CDCl_3): δ 6.66 (dd, 1H, $J = 2$, $J = 4$); 6.91–7.39 (m, 4H); 7.65 (s, 1H); 7.78–7.89 (m, 3H); 8.06 (d, 1H, $J = 2$); 8.75 (bs, 1H); 10.98 (bs, 1H).

Computational Methodologies. Calculations were performed on a Silicon Graphics O2 R10000 workstation. All the pyrazolo[4,3-*e*]1,2,4-triazolo[1,5-*c*]pyrimidine derivatives were constructed using the Molecule Builder module of Molecular Operating Environment (MOE 1998.10).⁴⁷ These structures were minimized using the MMFF94 force field,^{48–51} until the rms value of the truncated Newton method (TN) was <0.001 kcal/mol/Å. The optimized geometries of all pyrazolo[4,3-*e*]1,2,4-triazolo[1,5-*c*]pyrimidine structures were fully minimized using the RHF/AM1//RHF/3-21G(*) ab initio level of Gaussian 98.⁵² Atomic charges were calculated by fitting to electrostatic potential maps (CHELPG method).⁵³ Molecular volume and log *P* values (log of the octanol/water partition coefficient), a hydrophobicity indicator, were empirically calculated using the atom fragment method implemented in the QuaSAR-Descriptor module of MOE.⁴⁷

Biology. CHO Membranes Preparation. The expression of human A_1 , A_{2A} and A_3 receptors in CHO cells has been previously described.⁵⁴ The cells were grown adherently and maintained in Dulbecco's modified Eagle's medium with nutrient mixture F12 without nucleosides at 37 °C in 5% CO_2 /95% air. Cells were split two or three times weekly and then the culture medium was removed for membrane preparations. The cells were washed with phosphate-buffered saline and scrapped off into flasks in ice-cold hypotonic buffer (5 mM Tris HCl, 2 mM EDTA, pH 7.4). The cell suspension was homogenized with a Polytron and the homogenate was centrifuged for 30 min at 48000*g*. The membrane pellet was resuspended in 50 mM Tris HCl buffer at pH 7.4 for A_1 adenosine receptors, in 50 mM Tris HCl, 10 mM MgCl_2 at pH 7.4 for A_{2A} adenosine receptors, in 50 mM Tris HCl, and 10 mM MgCl_2 , 1 mM EDTA at pH 7.4 for A_3 adenosine receptors and were utilized for binding and adenylyl cyclase assays.

Human Cloned A_1 , A_{2A} , A_{2B} , and A_3 Adenosine Receptor Binding Assay. Binding of [^3H]DPCPX to CHO cells transfected with the human recombinant A_1 adenosine receptor was performed as previously described.⁴²

Displacement experiments were performed for 120 min at 25 °C in 0.20 mL of buffer containing 1 nM [^3H]DPCPX, 20 μL of diluted membranes (50 μg of protein/assay) and at least 6–8 different concentrations of examined compounds. Nonspecific binding was determined in the presence of 10 μM of CHA and this was always $\leq 10\%$ of the total binding.

Binding of [^3H]SCH 58261 to CHO cells transfected with the human recombinant A_{2A} adenosine receptors (50 μg of

protein/assay) was performed according to Varani et al.⁴⁶ In competition studies, at least 6–8 different concentrations of compounds were used and nonspecific binding was determined in the presence of 50 μM NECA for an incubation time of 60 min at 25 °C.

Binding of [^3H]DPCPX to HEK-293 cells (Receptor Biology Inc., Beltsville, MD) transfected with the human recombinant A_{2B} adenosine receptors was performed as already described.⁴² In particular, assays were carried out for 60 min at 25 °C in 0.1 mL of 50 mM Tris HCl buffer, 10 mM MgCl_2 , 1 mM EDTA, 0.1 mM benzamidine at pH 7.4, 2 IU/mL adenosine deaminase containing 40 nM [^3H]DPCPX, diluted membranes (20 μg of protein/assay) and at least 6–8 different concentration of tested compounds. Nonspecific binding was determined in the presence of 100 μM of NECA and was always $\leq 30\%$ of the total binding.

Binding of [^3H]MRE3008-F20 to CHO cells transfected with the human recombinant A_3 adenosine receptors was performed according to Varani et al.⁴² Competition experiments were carried out in duplicate in a finale volume of 250 μL in test tubes containing 1 nM [^3H]MRE3008-F20, 50 mM Tris HCl buffer, 10 mM MgCl_2 at pH 7.4, 100 μL of diluted membranes (50 μg protein/assay) and at least 6–8 different concentrations of examined ligands. Incubation time was 120 min at 4 °C, according to the results of previous time course experiments.⁴² Nonspecific binding was defined as binding in the presence of 1 μM of MRE3008-F20 and was about 25% of total binding. Bound and free radioactivity were separated by filtering the assay mixture through Whatman GF/B glass fiber filters using a Micro-Mate 196 cell harvester (Packard Instrument Co.). The filter bound radioactivity was counted on a Top Count (efficiency 57%) with Micro-Scint 20. The protein concentration was determined according to the Bio-Rad method⁵⁵ with bovine albumin as the reference standard.

Adenylyl Cyclase Assay. Membrane preparation was suspended in 0.5 mL of incubation mixture (50 mM Tris HCl, 10 mM MgCl_2 , 1 mM EDTA, pH 7.4) containing 5 μM GTP, 0.5 mM 4-(3-butoxy-4-methoxybenzyl)-2-imidazolidinone (Ro 20-1274) as phosphodiesterase inhibitor, 2.0 IU/mL adenosine deaminase and preincubated for 10 min in a shaking bath at 37 °C. Then IB-MECA or the antagonists examined plus ATP (1 mM) and forskolin 10 μM were added to the mixture and the incubation continued for a further 10 min. The potencies of antagonists were determined by antagonism of the IB-MECA (100 nM)-induced inhibition of cyclic AMP production. The reaction was terminated by transferring to a boiling water bath. Boiling was for 2 min, and then the tubes were cooled to room temperature and centrifuged at 2000*g* for 10 min at 4 °C. Supernatants (100 μL) were used in a competition protein binding assay carried out essentially according to Varani et al.⁴²

Samples of cyclic AMP standards (0–10 pmol) were added to each test tube containing the incubation buffer (0.1 M trizma base, 8.0 mM aminophylline, 6.0 mM 2-mercaptoethanol, pH 7.4) and [^3H]cyclic AMP in a total volume of 0.5 mL. The binding protein, previously prepared from beef adrenals, was added to the samples previously incubated at 4 °C for 150 min; after addition of charcoal the samples were centrifuged at 2000*g* for 10 min. The clear supernatant (0.2 mL) was mixed with 4 mL of Atomlight in a LS-1800 Beckman scintillation counter.

Acknowledgment. We thank Medco Research, Triangle Park, NC, for financial support, Dr. Kenneth A. Jacobson, NIH, Bethesda, MD, for use of the human A_3 adenosine receptor model in the creation of the pharmacophore maps, and Dr. Ennio Ongini, San Raffaele Scientific Park, Milan, Italy, for providing us with [^3H]SCH 58261.

References

- (1) Fredholm, B. B.; Abbracchio, M. P.; Burnstock, G.; Daly, J. W.; Harden, T. K.; Jacobson, K. A.; Leff, P.; Williams, M. Nomenclature and classification of purinoceptors. *Pharmacol. Rev.* **1994**, *46*, 143–156.

- (2) Olah, M. E.; Stiles, G. L. Adenosine receptor subtypes: characterization and therapeutic regulation. *Annu. Rev. Pharmacol. Toxicol.* **1995**, *35*, 581–606.
- (3) Jacobson, K. A.; Suzuki, F. Recent developments in selective agonists and antagonists acting at purine and pyrimidine receptors. *Drug. Dev. Res.* **1996**, *39*, 289–300.
- (4) Meyerhof, W.; Muller-Brechlin, R.; Richter, D. Molecular cloning of a novel putative G-protein coupled receptor expressed during rat spermiogenesis. *FEBS Lett.* **1991**, *284*, 155–160.
- (5) Sajjadi, F. G.; Firestein, G. S. cDNA cloning and sequence analysis of the human A₃ adenosine receptor. *Biochim. Biophys. Acta* **1993**, *1179*, 105–107.
- (6) Salvatore, C. A.; Jacobson, M. A.; Taylor, H. E.; Linden, J.; Johnson, R. G. Molecular cloning and characterization of the human A₃ adenosine receptor. *Proc. Natl. Acad. Sci. U.S.A.* **1993**, *90*, 10365–10369.
- (7) Linden, J. Cloned adenosine A₃ receptors: Pharmacological properties, species differences and receptor functions. *Trends Pharmacol. Sci.* **1994**, *15*, 298–306.
- (8) Zhao, Z. H.; Ravid, S.; Ravid, K. Chromosomal mapping of the mouse A₃ adenosine receptor gene, adora3. *Genomics* **1995**, *30*, 118–119.
- (9) Hill, R. J.; Oleynek, J. J.; Hoth, C. F.; Kiron, M. A.; Weng, W. F.; Wester, R. T.; Tracey, W. R.; Knight, D. R.; Buchholz, R.; Kennedy, S. P. Cloning, expression and pharmacological characterization of rabbit A₁ and A₃ receptors. *J. Pharmacol. Exp. Ther.* **1997**, *280*, 122–128.
- (10) Linden, J.; Taylor, H. E.; Robeva, A. S.; Tucker, A. L.; Stehle, J.; Rivkees, S. A.; Fink, J. S.; Reppert, S. M. Molecular cloning and functional expression of a sheep A₃ adenosine receptor with widespread tissue distribution. *Mol. Pharmacol.* **1993**, *44*, 524–532.
- (11) Hannon, J. P.; Pfannkuche, H. J.; Fozard, J. R. A role for mast cells in adenosine A₃ receptor-mediated hypotension in the rat. *Br. J. Pharmacol.* **1995**, *115*, 945–952.
- (12) Jacobson, K. A. Adenosine A₃ receptors: novel ligands and paradoxical effects. *Trends Pharmacol. Sci.* **1998**, *19*, 184–191.
- (13) Abbracchio, M. P.; Brambilla, R.; Kim, H. O.; von Lubitz, D. K. J. E.; Jacobson, K. A.; Cattabeni, F. G-protein-dependent activation of phospholipase-C by adenosine A₃ receptor in rat brain. *Mol. Pharmacol.* **1995**, *48*, 1038–1045.
- (14) Ali, H.; Choi, O. H.; Fraundorfer, P. F.; Yamada, K.; Gonzaga, H. M. S.; Beaven, M. A. Sustained activation of phospholipase-D via adenosine A₃ receptors is associated with enhancement of antigen-ionophore-induced and Ca²⁺-ionophore-induced secretion in a rat mast-cell line. *J. Pharmacol. Exp. Ther.* **1996**, *276*, 837–845.
- (15) van Schaick, E. A.; Jacobson, K. A.; Kim, H. O.; IJzerman, A. P.; Danhof, M. Haemodynamic effects and histamine release elicited by the selective adenosine A₃ receptor agonists 2-Cl-IB-MECA in conscious rats. *Eur. J. Pharmacol.* **1996**, *308*, 311–314.
- (16) von Lubitz, D. K. J.; Carter, M. F.; Deutsch, S. I.; Lin, R. C. S.; Mastropaolo, J.; Meshulam, J.; Jacobson, K. A. The effects of adenosine A₃ receptor stimulation on seizures in mice. *Eur. J. Pharmacol.* **1995**, *275*, 23–29.
- (17) von Lubitz, D. K. J. V.; Lin, R. C. S.; Popik, P.; Carter, M. F.; Jacobson, K. A. Adenosine A₃ receptor stimulation and cerebral ischemia. *Eur. J. Pharmacol.* **1994**, *263*, 59–67.
- (18) Mackenzie, W. M.; Hoskin, D. W.; Blay, J. Adenosine inhibits the adhesion of anti-CD3-activated killer lymphocytes to adenocarcinoma cells through an A₃ receptor. *Cancer Res.* **1994**, *54*, 3521–3526.
- (19) (a) Meade, C. J.; Mierau, J.; Leon, I.; Ensinger, H. A. In vivo role of the adenosine A₃ receptor-N⁶-2-(4-aminophenyl)ethyladenosine induces bronchospasm in bde rats by a neurally mediated mechanism involving cells resembling mast cells. *J. Pharmacol. Exp. Ther.* **1996**, *276*, 1148–1156. (b) Forsythe, P.; Ennis, M. Adenosine, mast cells and asthma. *Inflamm. Res.* **1999**, *48*, 301–307.
- (20) Ramkumar, V.; Stiles, G. L.; Beaven, M. A.; Ali, H. The A₃ adenosine receptors is the unique adenosine receptor which facilitates release of allergic mediators in mast cells. *J. Biol. Chem.* **1993**, *268*, 16887–16890.
- (21) Baraldi, P. G.; Cacciari, B.; Romagnoli, R.; Merighi, S.; Varani, K.; Borea, P. A.; Spalluto, G. A₃ Adenosine receptor ligands: history and perspectives. *Med. Res. Rev.* **2000**, *20*, 103–128.
- (22) van Rhee, A. M.; Jiang, J.-L.; Melman, N.; Olah, M. E.; Stiles, G. L.; Jacobson, K. A. Interaction of 1,4-dihydropyridine and pyridine derivatives with adenosine receptors: selectivity for A₃ receptors. *J. Med. Chem.* **1996**, *39*, 2980–2989.
- (23) Jiang, J.-L.; van Rhee, A. M.; Melman, N.; Ji, X.-D.; Jacobson, K. A. 6-Phenyl-1,4-dihydropyridine derivatives as potent and selective A₃ adenosine receptor antagonists. *J. Med. Chem.* **1996**, *39*, 4667–4675.
- (24) Jiang, J.-L.; van Rhee, A. M.; Chang, L.; Patchornik, A.; Ji, X.-D.; Evans, P.; Melman, N.; Jacobson, K. A. Structure–activity relationships of 4-(phenylethynyl)-6-phenyl-1,4-dihydropyridines as highly selective A₃ adenosine receptor antagonists. *J. Med. Chem.* **1997**, *40*, 2596–2608.
- (25) (a) Li, A.-H.; Moro, S.; Melman, N.; Ji, X.-D.; Jacobson, K. A. Structure–activity relationships and molecular modeling of 3,5-diacyl-2,4-dialkylpyridine derivatives as selective A₃ adenosine receptor antagonists. *J. Med. Chem.* **1998**, *41*, 3186–3201. (b) Li, A.-N.; Moro, S.; Forsyth, N.; Melman, N.; Ji, X.-D.; Jacobson, K. A. Synthesis, ComFA analysis and receptor docking of 3,5-diacyl-2,4-dialkylpyridine derivatives as selective A₃ adenosine receptor antagonists. *J. Med. Chem.* **1999**, *42*, 706–721.
- (26) Jiang, J.-L.; Li, A.-H.; Jang, S.-Y.; Chang, L.; Melman, N.; Moro, S.; Ji, X.-d.; Lokovsky, E. B.; Clardy, J. C.; Jacobson, K. A. Chiral resolution and stereospecificity of 6-phenyl-4-phenylethynyl-1,4-dihydropyridines as selective A₃ adenosine receptor antagonists. *J. Med. Chem.* **1999**, *42*, 3055–3065.
- (27) (a) Ji, X. D.; Melman, N.; Jacobson, K. A. Interactions of flavonoid and other phytochemicals with adenosine receptors. *J. Med. Chem.* **1996**, *39*, 398–406. (b) Karton, Y.; Jiang, J.-L.; Ji, X.-D.; Melman, N.; Olah, M. E.; Stiles, G. L.; Jacobson, K. A. Synthesis and biological activities of flavonoid derivatives as A₃ adenosine receptor antagonists. *J. Med. Chem.* **1996**, *39*, 2293–2301.
- (28) Moro, S.; van Rhee, A. M.; Sanders, L. H.; Jacobson, K. A. Flavonoid derivatives as adenosine receptor antagonists: a comparison of the hypothetical receptor binding site based on a comparative molecular field analysis model. *J. Med. Chem.* **1998**, *41*, 46–52.
- (29) van Muijlwijk-koezen, J. E.; Timmerman, H.; Link, R.; van der Goot, H.; IJzerman, A. P. A novel class of adenosine A₃ receptor ligands. 1. 3-(2-pyridinyl)isoquinoline derivatives. *J. Med. Chem.* **1998**, *41*, 3987–3993.
- (30) van Muijlwijk-koezen, J. E.; Timmerman, H.; Link, R.; van der Goot, H.; IJzerman, A. P. A novel class of adenosine A₃ receptor ligands. 2. Structure affinity profile of a series of isoquinoline and quinazoline compounds. *J. Med. Chem.* **1998**, *41*, 3994–4000.
- (31) van Muijlwijk-Koezen, J. E.; Timmerman, H.; van der Goot, H.; Menge, W. M. P. B.; von Frijtag von Drabbe Künzel, J. K.; de Groote, M.; IJzerman, A. P. Isoquinoline and quinazoline urea analogues as antagonists for the human adenosine A₃ receptor. *J. Med. Chem.* **2000**, *43*, 2227–2238.
- (32) Kim, Y. C.; Ji, X. D.; Jacobson, K. A. Derivatives of the triazoloquinazoline adenosine antagonist (CGS15943) are selective for the human A₃ receptor subtype. *J. Med. Chem.* **1996**, *39*, 4142–4148.
- (33) Kim, Y. C.; de Zwart, M.; Chang, L.; Moro, S.; Jacobien, K.; Frijtag, D. K.; Melman, N.; IJzerman, A. P.; Jacobson, K. A. Derivatives of the triazoloquinazoline adenosine antagonist (CGS15943) having high potency at the human A_{2B} and A₃ receptor subtypes. *J. Med. Chem.* **1998**, *41*, 2835–2845.
- (34) Baraldi, P. G.; Cacciari, B.; Romagnoli, R.; Spalluto, G.; Klotz, K.-N.; Leung, E.; Varani, K.; Gessi, S.; Merighi, S.; Borea, P. A. Pyrazolo[4,3-e]1,2,4-triazolo[1,5-c]pyrimidine derivatives as highly potent and selective human A₃ adenosine receptor antagonists. *J. Med. Chem.* **1999**, *42*, 4473–4478.
- (35) Baraldi, P. G.; Cacciari, B.; Spalluto, G.; Ji, X.-D.; Olah, M. E.; Stiles, G.; Dionisotti, S.; Zocchi, C.; Ongini, E.; Jacobson, K. A. Novel N⁶-(substituted-phenylcarbamoyl)adenosine-5'-uronamides as potent agonists for A₃ adenosine receptors. *J. Med. Chem.* **1996**, *39*, 802–806.
- (36) Baraldi, P. G.; Cacciari, B.; Pineda de Las Infantas, M. J.; Romagnoli, R.; Spalluto, G.; Volpini, R.; Costanzi, S.; Vittori, S.; Cristalli, G.; Melman, N.; Park, K.-S.; Ji, X.-D.; Jacobson, K. A. Synthesis and biological activity of a new series of N⁶-arylcarbamoyl, 2-(Ar)alkynyl-N⁶-arylcarbamoyl, and N⁶-carboxamido derivatives of adenosine-5'-N-ethyluronamide as A₁ and A₃ adenosine receptor agonists. *J. Med. Chem.* **1998**, *41*, 3174–3185.
- (37) Baraldi, P. G.; Manfredini, S.; Simoni, D.; Zappaterra, L.; Zocchi, C.; Dionisotti, S.; Ongini, E. Synthesis and activity of new pyrazolo[4,3-e]-1,2,4-triazolo[1,5-c]pyrimidine and 1,2,3-triazolo[4,5-e]-1,2,4-triazolo[1,5-c]pyrimidine displaying potent and selective activity as A_{2A} adenosine receptor antagonists. *Bioorg. Med. Chem. Lett.* **1994**, *4*, 2539–2544.
- (38) Baraldi, P. G.; Cacciari, B.; Spalluto, G.; Borioni, A.; Vizziano, M.; Dionisotti, S.; Ongini, E. Current developments of A_{2A} adenosine receptor antagonists. *Curr. Med. Chem.* **1995**, *2*, 707–722.
- (39) Baraldi, P. G.; Cacciari, B.; Spalluto, G.; Pineda de Las Infantas y Villatoro, M. J.; Zocchi, C.; Dionisotti, S.; Ongini, E. Pyrazolo[4,3-e]-1,2,4-triazolo[1,5-c]pyrimidine derivatives: Potent and selective A_{2A} adenosine antagonists. *J. Med. Chem.* **1996**, *39*, 1164–1171.

- (40) Baraldi, P. G.; Cacciari, B.; Spalluto, G.; Bergonzoni, M.; Dionisotti, S.; Ongini, E.; Varani, K.; Borea, P. A. Design, synthesis and biological evaluation of a second generation of pyrazolo[4,3-e]-1,2,4-triazolo[1,5-c]pyrimidines as potent and selective A_{2A} adenosine receptor antagonists. *J. Med. Chem.* **1998**, *41*, 2126–2133.
- (41) Lohse, M. J.; Klotz, K.-N.; Lindernborn-Fotinos, J.; Reddington, M.; Schwabe, U.; Olsson, R. A. 8-Cyclopentyl-1,3-dipropylxanthine DPCPX a selective high affinity antagonist radioligand for A₁ adenosine receptors. *Naunyn-Schmiedeberg's Arch. Pharmacol.* **1987**, *336*, 204–210.
- (42) Varani, K.; Merighi, S.; Gessi, S.; Klotz, K. N.; Leung, E.; Baraldi, P. G.; Cacciari, B.; Spalluto, G.; Borea, P. A. [³H]MRE3008-F20: a novel antagonist radioligand for the pharmacological and biochemical characterization of human A₃ adenosine receptors. *Mol. Pharmacol.* **2000**, *57*, 968–975.
- (43) Zocchi, C.; Ongini, E.; Ferrara, S.; Baraldi, P. G.; Dionisotti, S. Binding of the radioligand [³H]-SCH58261, a new nonxanthine A_{2A} adenosine receptor antagonist, to rat striatal membranes. *Br. J. Pharmacol.* **1996**, *117*, 1381–1386.
- (44) Baraldi, P. G.; Cacciari, B.; Romagnoli, R.; Varani, K.; Merighi, S.; Gessi, S.; Borea, P. A.; Leung, E.; Hickey, S. L.; Spalluto, G. Synthesis and preliminary biological evaluation of [³H]MRE3008-F20: the first high affinity radioligand antagonist for the human A₃ adenosine receptors. *Bioorg. Med. Chem. Lett.* **2000**, *10*, 209–211.
- (45) Moro, S.; Li, A. H.; Jacobson, K. A. Molecular modeling studies of human A₃ adenosine antagonists: structural homology and receptor docking. *J. Chem. Inf. Comput. Sci.* **1998**, *38*, 1239–1248.
- (46) Varani, K.; Gessi, S.; Dionisotti, S.; Ongini, E.; Borea, P. A. [³H]-SCH 58261 Labeling of functional A_{2A} adenosine receptors in human neutrophil membranes. *Br. J. Pharmacol.* **1998**, *123*, 1723–1731.
- (47) Molecular Operating Environment (MOE 1999.05); Chemical Computing Group, Inc., 1255 University St., Suite 1600, Montreal, Quebec H3B 3X3, Canada.
- (48) Halgren, T. Merck Molecular Force Field. I. Form, Scope, Parametrization and Performance of MMFF94. *J. Comput. Chem.* **1996**, *17*, 490–519.
- (49) Halgren, T. Merck Molecular Force Field. II. MMFF94 van der Waals and Electrostatic Parameters for Intermolecular Interaction. *J. Comput. Chem.* **1996**, *17*, 520–552.
- (50) Halgren, T. Merck Molecular Force Field. III. Molecular Geometries and Vibrational frequencies for MMFF94. *J. Comput. Chem.* **1996**, *17*, 553–586.
- (51) Halgren, T. Merck Molecular Force Field. IV. Conformational Energies and Geometries for MMFF94. *J. Comput. Chem.* **1996**, *17*, 587–615.
- (52) Halgren, T.; Nachbar, R. Merck Molecular Force Field. V. Extension of MMFF94 Using Experimental Data, Additional Computational Data, and Empirical Rules. *J. Comput. Chem.* **1996**, *17*, 616–632.
- (53) Frisch, M.; Trucks, G. W.; Schlegel, H.; Scuseria, G.; Robb, M.; Cheeseman, J.; Zakrzewski, V.; Montgomery, J.; Stratmann, R. E.; Burant, J. C.; Dapprich, S.; Millam, J.; Daniels, A.; Kudin, K.; Strain, M.; Farkas, O.; Tomasi, J.; Barone, V.; Cossi, M.; Cammi, R.; Mennucci, B.; Pomelli, C.; Adamo, C.; Clifford, S.; Ochterski, J.; Petersson, G. A.; Ayala, P. Y.; Cui, Q.; Morokuma, K.; Malick, D. K.; Rabuck, A. D.; Raghavachari, K.; Foresman, J. B.; Cioslowski, J.; Ortiz, J. V.; Stefanov, B. B.; Liu, G.; Liashenko, A.; Piskorz, P.; Komaromi, I.; Gomperts, R.; Martin, R. L.; Fox, D. J.; Keith, T.; Al-Laham, M. A.; Peng, C. Y.; Nanayakkara, A.; Gonzalez, C.; Challacombe, M.; Gill, P. M. W.; Johnson, B. G.; Chen, W.; Wong, M. W.; Andres, J. L.; Head-Gordon, M.; Replogle, E. S.; Pople, J. A. Gaussian 98, revision A.6; Gaussian, Inc., Pittsburgh, PA, 1998.
- (54) Klotz, K. N.; Hessling, J.; Hegler, J.; Owman, C.; Kull, B.; Fredholm, B. B.; Lohse, M. J. Comparative pharmacology of human adenosine receptor subtypes- characterization of stably transfected receptors in CHO cells. *Naunyn-Schmiedeberg's Arch. Pharmacol.* **1998**, *357*, 1–9.
- (55) Bradford, M. M. A rapid sensitive method for the quantification of microgram quantities of protein utilizing the principle of protein dye-binding. *Anal. Biochem.* **1976**, *72*, 248–254.

JM001047Y